Flexible aliphatic diammonioacetates as zwitterionic ligands in UO2 2+ complexes: Diverse topologies and interpenetrated structures

Sotaro Kusumoto, Youssef Atoini, Shunya Masuda, Yoshihiro Koide, Jee Young Kim, Shinya Hayami, Yang Kim, Jack Harrowfield, Pierre Thuéry

Flexible Aliphatic Diammonioacetates as Zwitterionic Ligands in UO_2^{2+} Complexes: Diverse Topologies and Interpenetrated Structures

Sotaro Kusumoto,[a] Youssef Atoini,[b] Shunya Masuda,[a] Yoshihiro Koide,[a] Jee Young Kim,[c] Shinya Hayami,*[,d] Yang Kim,*[,d] Jack Harrowfield,*[,e] and Pierre Thuéry*[,f]

[a] Department of Material & Life Chemistry, Kanagawa University, 3-27-1 Rokkakubashi, Kanagawa-ku, Yokohama 221-8686, Japan

[b] Technical University of Munich, Campus Straubing, Schulgasse 22, 94315 Straubing, Germany

[c] Department of Food and Nutrition, Kosin University, 194 Wachiro, Yongdo-Gu, Busan 49104, South Korea

[d] Department of Chemistry, Graduate School of Science and Technology, Institute of Industrial Nanomaterials (IINa), Kumamoto University, 2-39-1 Kurokami, Chuo-ku, Kumamoto 860-8555, Japan

[e] Université de Strasbourg, ISIS, 8 allée Gaspard Monge, 67083 Strasbourg, France

[f] Université Paris-Saclay, CEA, CNRS, NIMBE, 91191 Gif-sur-Yvette, France

ABSTRACT: *N,N,N′,N′*-Tetramethylethane-1,2-diammonioacetate (L1) and *N,N,N′,N′*-tetramethylpropane-1,3-diammonioacetate (L2) are two flexible zwitterionic dicarboxylates which have been used as ligands for the uranyl ion, 12 complexes having been obtained from their coupling to diverse anions, mostly anionic polycarboxylates, or oxo, hydroxo and chlorido donors. The protonated zwitterion is a simple counterion in $[H_2L1][UO_2(2,6\text{-pydc})_2]$ (**1**), where 2,6-pydc^{2-} is 2,6-pyridinedicarboxylate, but it is deprotonated and coordinated in all the other complexes. $[(UO_2)_2(L2)(2,4\text{-pydcH})_4]$ (**2**), where 2,4-pydc^{2-} is 2,4-pyridinedicarboxylate, is a discrete, binuclear complex due to the terminal nature of the partially deprotonated anionic ligands. $[(UO_2)_2(L1)(ipht)_2]\cdot 4H_2O$ (**3**) and $[(UO_2)_2(L1)(pda)_2]$ (**4**), where ipht^{2-} and pda^{2-} are isophthalate and 1,4-phenylenediacetate, are monoperiodic coordination polymers in which central L1 bridges connect two lateral strands. Oxalate anions (ox^{2-}) generated *in situ* give $[(UO_2)_2(L1)(ox)_2]$ (**5**), a diperiodic network with the **hcb** topology. $[(UO_2)_2(L2)(ipht)_2]\cdot H_2O$ (**6**) differs from **3** in being a diperiodic network with the V_2O_5 topological type. $[(UO_2)_2(L1)(2,5\text{-pydc})_2]\cdot 4H_2O$ (**7**), where 2,5-pydc^{2-} is 2,5-pyridinedicarboxylate, is a **hcb** network with a square-wave profile, while $[(UO_2)_2(L1)(dnhpa)_2]$ (**8**), where dnhpa^{2-} is 3,5-dinitro-2-hydroxyphenoxyacetate, formed *in situ* from 1,2-phenylenedioxydiacetic acid, has the same topology but a strongly corrugated shape leading to interdigitation of layers. (2*R*,3*R*,4*S*,5*S*)-tetrahydrofurantetracarboxylic acid (thftcH$_4$) is only partially deprotonated in $[(UO_2)_3(L1)(thftcH)_2(H_2O)]$ (**9**), which crystallizes as a diperiodic polymer with the **fes** topology. $[(UO_2)_2Cl_2(L1)_3][(UO_2Cl_3)_2(L1)]$ (**10**) is an ionic compound in which discrete, binuclear anions cross the cells of the cationic **hcb** network. 2,5-Thiophenediacetate (tdc^{2-}) is peculiar in promoting self-sorting of the ligands in the ionic complex $[(UO_2)_5(L1)_7(tdc)(H_2O)][(UO_2)_2(tdc)_3]_4\cdot CH_3CN\cdot 12H_2O$ (**11**), which is the first example of hetero-interpenetration in uranyl chemistry, involving a triperiodic, cationic framework and diperiodic, anionic **hcb** networks. Finally, $[(UO_2)_7(O)_3(OH)_{4.3}Cl_{2.7}(L2)_2]Cl\cdot 7H_2O$ (**12**) crystallizes as a twofold interpenetrated, triperiodic framework in which chlorouranate undulating monoperiodic subunits are bridged by the L2 ligands. Complexes **1**, **2**, **3** and **7** are emissive with photoluminescence quantum yields in the range of 8–24%, and their solid state emission spectra show the usual dependence on number and nature of donor atoms.

INTRODUCTION

A particularly appealing line of investigation in the study of metal–organic frameworks (MOFs) is the design of mixed-ligand (and more generally mixed-component) species, with the prospect of thus generating multifunctional materials.[1–3] Although quite sophisticated strategies have been used to synthesize mixed-ligand coordination polymers, generally under solvo- or hydrothermal conditions, the most straightforward consists in simply using a mixture of the desired ligands, leading to their statistical or ordered distribution over the several coordination sites. In the subclass of MOFs in which the metal cation used is the uranyl ion UO_2^{2+} (UOFs),[4–8] some early examples involved ligands containing different donor groups, such as dicarboxylates and divergent dipyridine derivatives, very different in terms of donor strength.[9,10] In contrast, attempts at synthesis of coordination polymers containing different bridging anionic polycarboxylates most often proved disappointing, resulting in only one of the ligands being incorporated in the complex (with the exception of very simple ligands such as oxalate); in our experience, mixed-ligand species were only obtained with polycarboxylates close to each other, such as the *cis* and *trans* isomers of 1,2-, 1,3- and 1,4-cyclohexanedicarboxylates,[11,12] or the positional isomers 1,2- and 1,4-phenylenediacetates.[13] However, we have found recently that one way to obtain the desired mixed-ligand uranyl ion coordination polymers is to use a mixture of anionic and zwitterionic polycarboxylates, in part possibly as a result of a decrease of electrostatic repulsions in the metal coordination sphere compared with the case in which all ligands are anionic, but also as a consequence of limiting the number of anionic carboxylate donors in the reaction mixtures to less than that required for $[UO_2(RCO_2)_3]^-$ species. This has been demonstrated in the case of several anionic polycarboxylates of different size, shape and denticity with either the metal-containing zwitterionic carboxylate $Ni(tpyc)_2$ ($tpyc^-$ = 2,2′;6′,2″-terpyridine-4′-carboxylate)[14,15] or the aromatic derivatives 1,1′-[(2,3,5,6-tetramethylbenzene-1,4-diyl)bis(methylene)]bis(pyridin-1-

ium-*n*-carboxylate) (*n* = 3 or 4), and 1,1′,1″-[(2,4,6-trimethylbenzene-1,3,5-triyl)tris(methylene)]tris(pyridin-1-ium-4-carboxylate).[16,17] This strategy consisting in combining ligands very different in terms of size, geometry and flexibility, but of similar donor strength,[17] has generated some original structures, such as polynuclear rings,[15,16] and entangled polymers,[16] and thus has induced attempts to extend this investigation to other zwitterionic dicarboxylates. We report herein our results with two flexible diammonioacetates, *N,N,N′,N′*-tetramethylethane-1,2-diammonioacetate (L1) and *N,N,N′,N′*-tetramethylpropane-1,3-diammonioacetate (L2), represented in Scheme 1. Combining one or the other of these ligands

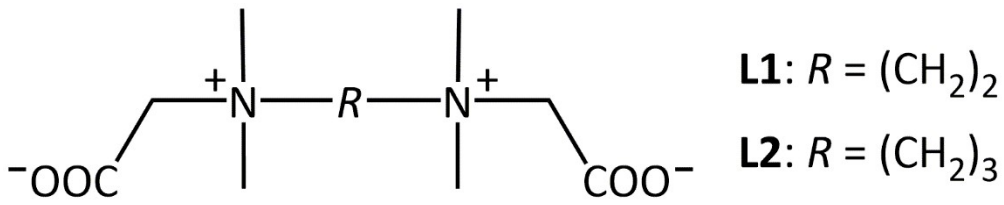

Scheme 1. The Zwitterionic Carboxylate Ligands L1 and L2

mainly with various dicarboxylic acids has given a series of 12 complexes which have been characterized by their crystal structure and, when possible, their photoluminescence properties in the solid state. These zwitterionic species have seldom been used in coordination chemistry, the Cambridge Structural Database (CSD, Version 5.43)[18,19] giving as the only reported crystal structures those of the Na^+ and Hg^{II} complexes of both L1 and L2,[20,21] and of three lanthanide cation complexes of L2,[22,23] but none involving actinide cations, nor a mixture with anionic carboxylate ligands. The complexes described herein with these non-aromatic ligands of enhanced flexibility display variable periodicities and they range from discrete, molecular complexes to triperiodic frameworks, the latter providing a novel example of framework interpenetration and a unique case of hetero-interpenetration[24–27] in uranyl chemistry.

EXPERIMENTAL SECTION

Syntheses. ***Caution!*** *Uranium is a radioactive and chemically toxic element, and uranium-containing samples must be handled with suitable care and protection. Small quantities of reagents and solvents were employed to minimize any potential hazards arising both from the presence of uranium and the use of pressurized vessels for the syntheses.*

$[UO_2(NO_3)_2(H_2O)_2]\cdot 4H_2O$ (RP Normapur, 99%) was purchased from Prolabo, and the carboxylic acids were from Aldrich. ^{1}H NMR spectra of $L1H_2Cl_2$ and $L2H_2Cl_2$ (D_2O solvent) were recorded on a JEOL 400 MHz spectrometer and they are given in Figure S1 (Supporting Information). Elemental analyses of $L1H_2Cl_2$ and $L2H_2Cl_2$ have not been performed because both zwitterionic ligands are very hygroscopic. Elemental analyses of the uranyl ion complexes were made by MEDAC Ltd.

Syntheses of the zwitterionic ligand precursors (protonated forms). Both $L1H_2Cl_2$ and $L2H_2Cl_2$ were prepared by slight modifications of the method reported in the literature.[28]

$L1H_2Cl_2$. *N,N,N′,N′*-Tetramethylethylenediamine (20 mmol, 2.33 g) and ethylchloroacetate (43 mmol, 5.27 g) were mixed in ethanol (10 mL) and heated under reflux for 1 h. The solvent was removed under reduced pressure before adding HCl (3.6%, 20 mL) and again heating under reflux for 3 h. The mixture was evaporated under reduced pressure to give a gelatinous solid, which was then triturated with ethanol (20 mL) to give a white powder. The product was filtered off and washed with ethanol, and dried under vacuum. Yield: 1.44 g (31 %). ^{1}H NMR (400 MHz, D_2O): δ = 3.22 (s, 12H), 4.03 (s, 4H), 4.14 (s, 4H).

$L2H_2Cl_2$. $L2H_2Cl_2$ was prepared in the same way as $L1H_2Cl_2$ except for the use of *N,N,N′,N′*-tetramethyl-1,3-propanediamine (20 mmol, 2.60 g) instead of *N,N,N′,N′*-tetramethylethylenediamine. Yield: 1.67 g (34 %). ^{1}H NMR (400 MHz, D_2O): δ = 2.12 (quin, 2H), 3.17 (s, 4H), 3.54 (t, 4H), 4.03 (s, 4H).

Uranyl Ion Complex Syntheses. For the syntheses of all complexes, a mixture of $[UO_2(NO_3)_2(H_2O)_2]\cdot 4H_2O$ (25 mg, 0.05 mmol), H_2L1Cl_2 or H_2L2Cl_2 (0.05 mmol), and the additional carboxylic acid (0.05 mmol) were dissolved in a mixture of water (0.6 mL) and acetonitrile (0.2 mL). The solutions were placed in 10 mL tightly closed glass vessels (Pyrex® culture tubes with SVL15 stoppers and Teflon-coated seals, provided by VWR) and heated at 140 °C in a sand bath (Harry Gestigkeit ST72), and the crystals, of light yellow or yellow-green color, were grown in the hot, pressurized solutions (and not as a result of a final return to ambient conditions) after about 24 h to 3 w, the longest times being for complexes **5** and **12**. The carboxylic acids used are represented in Scheme 2, and a summary of the complexes obtained is given in Table 1. The reaction times, yields and results of elemental analyses are given in Table S1 (Supporting Information). Complex **5**, involving the oxalate ligand, was obtained three times, with *cis*-muconic acid, 4-ketopimelic acid, or CsI used as additional reagents, the oxalate anion being generated *in situ*, as frequently observed in such solvo-hydrothermal syntheses.[29,30] In this synthesis and that of **12**, CsI was added as a possible source of triiodide anion.[14] During the synthesis of complex **8**, 1,2-phenylenedioxydiacetic acid underwent partial decomposition, with cleavage of one ether group to give a phenol susceptible to nitration under the reaction conditions, resulting in the formation of 3,5-dinitro-2-hydroxyphenoxyacetic acid ($dnhpaH_2$).

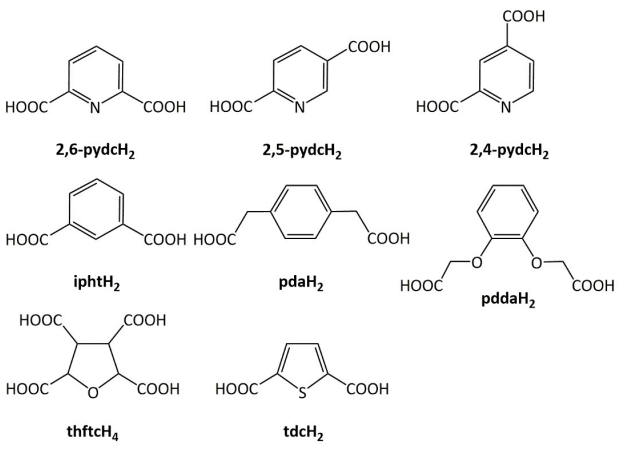

Scheme 2. Polycarboxylic Acids Used as Coligands

Table 1. Summary of the Complexes Obtained

compound	additional carboxylic acid/reagent
$[H_2L1][UO_2(2,6\text{-pydc})_2]$ (**1**)	2,6-pyridinedicarboxylic acid (2,6-pydcH_2)
$[(UO_2)_2(L2)(2,4\text{-pydcH})_4]$ (**2**)	2,4-pyridinedicarboxylic acid (2,4-pydcH_2)
$[(UO_2)_2(L1)(ipht)_2]\cdot 4H_2O$ (**3**)	isophthalic acid (iphtH_2)
$[(UO_2)_2(L1)(pda)_2]$ (**4**)	1,4-phenylenediacetic acid (pdaH_2)
$[(UO_2)_2(L1)(ox)_2]$ (**5**)	oxalic acid (oxH_2, generated *in situ*)
$[(UO_2)_2(L2)(ipht)_2]\cdot H_2O$ (**6**)	isophthalic acid (iphtH_2)
$[(UO_2)_2(L1)(2,5\text{-pydc})_2]\cdot 4H_2O$ (**7**)	2,5-pyridinedicarboxylic acid (2,5-pydcH_2)
$[(UO_2)_2(L1)(dnhpa)_2]$ (**8**)	1,2-phenylenedioxydiacetic acid (pddaH_2)
$[(UO_2)_3(L1)(thftcH)_2(H_2O)]$ (**9**)	(2*R*,3*R*,4*S*,5*S*)-tetrahydrofurantetracarboxylic acid (thftcH_4)
$[(UO_2)_2Cl_2(L1)_3][(UO_2Cl_3)_2(L1)]$ (**10**)	terephthalic acid
$[(UO_2)_5(L1)_7(tdc)(H_2O)][(UO_2)_2(tdc)_3]_4\cdot CH_3CN\cdot 12H_2O$ (**11**)	2,5-thiophenedicarboxylic acid (tdcH_2)
$[(UO_2)_7(O)_3(OH)_{4.3}Cl_{2.7}(L2)_2]Cl\cdot 7H_2O$ (**12**)	CsI

Crystallography. The data were collected at 100(2) K on a Bruker D8 Quest diffractometer equipped with an Incoatec microfocus source (IμS 3.0 Mo, λ = 0.71073 Å) and a PHOTON III area detector, and operated through the APEX3 software.[31] The crystals were mounted on Mitegen micromounts with a protective coating of Paratone-N oil (Hampton Research). The data were processed with SAINT[32] and empirical absorption corrections (multi-scan) were made with SADABS.[33,34] All structures were solved by intrinsic phasing with SHELXT,[35] and refined by full-matrix least-squares on F^2 with SHELXL,[36] using the ShelXle interface.[37] All non-hydrogen atoms were refined with anisotropic displacement parameters. When possible, the hydrogen atoms bound to oxygen atoms were retrieved from residual electron density maps, and they were refined, either freely or with restraints on bond lengths and angles when necessary. The carbon-bound hydrogen atoms were introduced at calculated positions and were treated as riding atoms with an isotropic displacement parameter equal to 1.2 times that of the parent atom (1.5 for CH_3). Some voids in the structures of compounds **6**, **11** and **12** contain disordered solvent molecules which could not be modelled satisfactorily, and the SQUEEZE software[38] was used to subtract their contribution to the structure factors. In

compound **9**, the thftc ring is partly disordered over two positions, one of them largely dominant, which have been refined with occupancy parameters constrained to sum to unity and some restraints on bond lengths and displacement parameters. In compound **12**, one chloride anion (Cl2) and one hydroxide anion (O16) are disordered over close positions corresponding to the same coordination site, and their occupancy parameters have first been refined, then fixed to 0.35 and 0.15, respectively; another, uncoordinated chloride anion is disordered over two sites, with a global occupancy of 0.5, a water molecule with an occupancy parameter of 0.5 being located close to one of these positions. Crystal data and structure refinement parameters are given in Table 2. The molecular plots were drawn with ORTEP-3,[39,40] and the polyhedral representations with VESTA.[41] The topological analyses and nodal representations were made with ToposPro.[42]

Luminescence Measurements. Emission spectra were recorded on solid samples using an Edinburgh Instruments FS5 spectrofluorimeter equipped with a 150 W CW ozone-free xenon arc lamp, dual-grating excitation and emission monochromators (2.1 nm/mm dispersion; 1200 grooves/mm) and an R928P photomultiplier detector. The powdered compounds were pressed to the wall of a quartz tube, and the measurements were performed using the right-angle mode in the SC-05 cassette. An excitation wavelength of 420 nm was used in all cases and the emission was monitored between 450 and 600 nm. The quantum yield measurements were performed by using a Hamamatsu Quantaurus C11347 absolute photoluminescence quantum yield spectrometer and exciting the samples between 300 and 400 nm.

Table 2. Crystal Data and Structure Refinement Details

	1	2	3	4	5	6
chemical formula	$C_{24}H_{28}N_4O_{14}U$	$C_{39}H_{38}N_6O_{24}U_2$	$C_{26}H_{36}N_2O_{20}U_2$	$C_{30}H_{36}N_2O_{16}U_2$	$C_{14}H_{20}N_2O_{16}U_2$	$C_{27}H_{32}N_2O_{17}U_2$
M (g mol^{-1})	834.53	1450.81	1172.63	1156.67	948.38	1132.60
cryst syst	monoclinic	monoclinic	monoclinic	triclinic	triclinic	triclinic
space group	$P2_1/c$	$P2_1/c$	$P2_1/n$	$P\bar{1}$	$P\bar{1}$	$P\bar{1}$
a (Å)	11.2988(5)	18.6592(7)	9.9049(6)	6.6125(3)	6.0581(3)	9.7779(6)
b (Å)	7.8882(3)	13.5859(4)	12.3281(8)	8.9425(3)	9.6374(6)	10.9807(7)
c (Å)	15.6575(7)	17.3012(6)	14.1215(11)	14.3776(5)	10.1631(6)	16.8464(10)
α (deg)	90	90	90	90.4077(15)	70.8640(18)	99.645(2)
β (deg)	101.9070(16)	98.1744(14)	105.872(2)	96.3031(14)	85.607(2)	90.173(3)
γ (deg)	90	90	90	97.9469(14)	86.1093(18)	95.936(2)
V (Å^3)	1365.48(10)	4341.3(3)	1658.6(2)	836.71(6)	558.36(6)	1773.26(19)
Z	2	4	2	1	1	2
reflns collcd	85766	154204	33552	44321	23691	58115
indep reflns	2570	13240	3149	4301	2056	6736
obsd reflns [$I > 2\sigma(I)$]	2422	12361	2845	4098	2000	5788
R_{int}	0.044	0.044	0.052	0.054	0.040	0.063
params refined	201	660	240	228	156	437
R_1	0.018	0.017	0.022	0.019	0.020	0.026
wR_2	0.047	0.038	0.047	0.042	0.048	0.060
$\Delta\rho_{min}$ (e Å^{-3})	–0.63	–0.85	–1.89	–1.81	–1.52	–1.67
$\Delta\rho_{max}$ (e Å^{-3})	2.32	1.34	1.34	1.28	1.37	1.18

	7	8	9	10	11	12
chemical formula	$C_{24}H_{34}N_4O_{20}U_2$	$C_{26}H_{28}N_6O_{24}U_2$	$C_{26}H_{34}N_2O_{30}U_3$	$C_{40}H_{80}Cl_8N_8O_{24}U_4$	$C_{152}H_{198}N_{16}O_{119}S_{13}U_{13}$	$C_{22}H_{62.3}Cl_{3.7}N_4O_{36.3}U_7$
M (g mol^{-1})	1174.61	1284.60	1568.64	2292.84	7664.42	2761.23
cryst syst	monoclinic	orthorhombic	triclinic	monoclinic	monoclinic	orthorhombic
space group	$C2/c$	$Pbca$	$P\bar{1}$	$P2_1/n$	$C2/c$	$Ibca$
a (Å)	15.6224(4)	8.7580(3)	8.7330(3)	9.6502(3)	18.2570(6)	19.6732(6)
b (Å)	12.6502(4)	12.7959(5)	10.8683(3)	21.1882(5)	33.0624(10)	21.7697(5)
c (Å)	16.7667(4)	30.9029(13)	10.9649(3)	16.4749(5)	38.0299(14)	27.0581(7)
α (deg)	90	90	116.3145(10)	90	90	90
β (deg)	103.7980(10)	90	98.2599(11)	102.7473(12)	101.9363(16)	90
γ (deg)	90	90	90.1270(12)	90	90	90
V (Å^3)	3217.92(15)	3463.2(2)	920.64(5)	3285.60(16)	22459.3(13)	11588.4(5)
Z	4	4	1	2	4	8
reflns collcd	37690	48776	27182	98342	126349	125096
indep reflns	4164	5295	3478	9973	21307	5506
obsd reflns [$I > 2\sigma(I)$]	3685	4329	3347	9308	17722	5256
R_{int}	0.056	0.067	0.040	0.045	0.070	0.056
params refined	234	264	316	387	1426	368
R_1	0.023	0.026	0.031	0.018	0.032	0.024
wR_2	0.052	0.057	0.073	0.038	0.074	0.058
$\Delta\rho_{min}$ (e Å^{-3})	–0.98	–1.16	–1.75	–1.09	–3.38	–0.87
$\Delta\rho_{max}$ (e Å^{-3})	1.20	1.67	2.96	1.88	1.52	1.52

RESULTS AND DISCUSSION

Although the metal/zwitterion/polycarboxylate stoichiometry chosen for the syntheses was 1:1:1, with the intent of obtaining the zwitterion bound to a neutral polymer, it is not retained in any of the crystallized complexes. In the case of anionic dicarboxylates, the 2:1:2 stoichiometry is the large favorite, being found in complexes **3**–**8** and giving neutral species. The same organic cosolvent, acetonitrile, was used in all cases, and it is only present as a solvent in complex **11**, with neither of its hydrolysis products, ammonium and acetate ions, being present in any species. As a general trend, the added anionic polycarboxylate is included as a

ligand as intended, but for the cases of complex **5**, in which oxalate generated *in situ* is present instead, complex **8**, in which pddaH$_2$ reacted to give dnhpaH$_2$ (see Experimental Section), and complex **10**, in which terephthalic acid is absent altogether, being displaced by coordinated chloride anions. No anionic carboxylate is present in **12**, this complex having been obtained in the presence of CsI so as to possibly form the bulky I_3^- counterion, as previously reported,[14] coordinated chloride anions being however incorporated instead. These particular variations in the nature of the isolated materials, only some of those known for solvothermal syntheses,[43] provide intriguing glimpses of the complicated solution chemistry of uranyl ion under solvothermal conditions. Our use of pressure-resistant but transparent reaction glass vessels leaves open the prospect of U^{VI} photooxidations and it is known from studies under ambient conditions[44] that both ether and alkene units are especially susceptible to attack by photo-excited uranyl ion (the initial step being hydrogen abstraction to give the ligand radical), possibly explaining the presence of oxalate in complex **5**, although its presence in the case where only CsI was added to the reaction mixture along with the zwitterion source shows that the latter must also be an oxidisable carbon source. A different zwitterion has also been shown to undergo conversion to oxalate on reaction in an autoclave presumably shut off from light[45] and we have shown elsewhere that it is possible to obtain both muconate[46] and ketopimelate[16] complexes under the present conditions, so we are inclined to discount photocatalytic oxidation as an important influence, although in one instance we have isolated a product explicable in terms of a radical coupling process[47] and in general it could be a cause of reduction in yields. The convenience of the use of hydrated uranyl nitrate as a source of uranyl ion of course guarantees the presence of a strong thermal oxidant, nitrate, in the reaction mixtures and acid-catalyzed ether cleavage to give readily oxidized alcohols could be an alternative pathway to the oxalate found commonly in systems involving crown ethers[48] to that involving reductive coupling of CO_2 produced via carboxylic acid decarboxylation.[29,30] The cleavage of one ether

arm of 1,2-phenylenedioxydiacetic acid to give an activated (phenolic) aromatic centre able to undergo dinitration as seen in complex **8** may also be seen as a warning of the potential danger of the presence of nitrate, in addition to the implication that the results of solvothermal syntheses could well be quite different with uranyl triflate, for example, as an alternative source to the nitrate.

No deviation of the uranium atom environment from the usual pentagonal- or hexagonal-bipyramidal geometries (sometimes coexisting in the same crystal) is observed over the whole series, the O_5 equatorial environment being the most common (complexes **4**–**6**, **8**, **9**, **11** and **12**), followed by O_6 (**3**, **9** and **11**), and the mixed-donor sets O_3N_2 (**2**), O_4Cl and/or O_2Cl_3 (**10** and **12**), O_4N_2 (**1**), and O_5N (**7**). The associated bond lengths are also unexceptional, being in the ranges 1.753(4)–1.801(6) Å for U=O, 2.2835(14)–2.462(4) Å for monodentate zwitterionic carboxylates, 2.434(5)–2.5740(16) Å for κ^2O,O'-chelating zwitterionic carboxylates, 2.241(2)–2.4940(17) Å for monodentate anionic carboxylates, and 2.421(2)–2.511(4) Å for κ^2O,O'-chelating anionic carboxylates. The crystal structures will be described in the order of increasing periodicity.

Molecular complexes. $[H_2L1][UO_2(2,6\text{-pydc})_2]$ (**1**) is the only case in which the zwitterionic precursor is not deprotonated and remains uncoordinated, the uranium atom, located on an inversion centre, being chelated in the ONO site of two 2,6-$pydc^{2-}$ ligands (Figure 1). This may in part be due to the particular stability of the $UO_2(2,6\text{-pydc})_2^{2-}$ moiety, which is found in 24 complexes reported in the CSD, but the 1:1 complex $[UO_2(2,6\text{-pydc})(H_2O)]$ has long been known[49] and the formation constants for two complexes in aqueous solution at 298 K provide no evidence of cooperativity,[50] so that the isolation of the 1:2 complex from a 1:1 mixture may simply reflect the exceptionally low solubility of the crystal. The counterion is the centrosymmetric, diprotonated H_2L1^{2+}, which forms two hydrogen bonds with uncoordinated

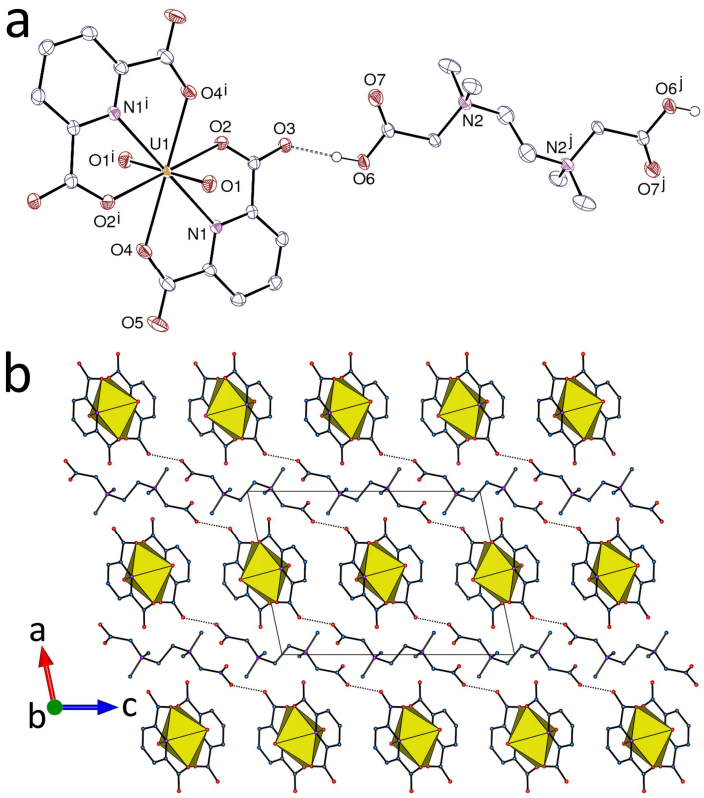

Figure 1. (a) View of compound **1**. Displacement ellipsoids are drawn at the 50% probability level. Carbon-bound hydrogen atoms are omitted and the hydrogen bond is shown as a dashed line. Symmetry codes: i = 1 – *x*, –*y*, 1 – *z*; j = 2 – *x*, 1 – *y*, –*z*. (b) View of the packing with hydrogen bonded cations and anions. Uranium coordination polyhedra are colored yellow and hydrogen bonds are shown as dotted lines.

carboxylate oxygen atoms pertaining to two different anions, thus forming chains parallel to [11$\bar{1}$], while the packing shows alternate sheets of anions and cations parallel to (100). Within stacks parallel to (001), the anionic units are associated through parallel-displaced π-stacking interactions [centroid···centroid distance, 4.0714(15) Å; dihedral angle, 0°], which are possibly associated with weak interactions between uranyl oxo groups and aromatic rings [shortest O···C(arom) distance, 3.003(3) Å], as in the alkali metal ion analogues.[50,51] These interactions are apparent on the Hirshfeld surfaces (HSs)[52] calculated with CrystalExplorer (ver. 3.1).[53] The packing is quite compact and no solvent-accessible space is present, as indicated by the Kitaigorodski packing index (KPI, calculated with PLATON[54]) of 0.73.

From a reaction mixture containing the isomeric 2,4-pyridinedicarboxylic acid, incapable of tridentate bonding to a single uranyl centre (as its dianion), and the zwitterion precursor H_2L2Cl_2, the isolated complex, $[(UO_2)_2(L2)(2,4\text{-pydcH})_4]$ (**2**), proved to contain the true zwitterion bound as a bis(κ^1O) bridge between uranyl ions. The singly-deprotonated 2,4-pydcH$^-$ anion is bound as an N,O-chelate, four such ligands being necessary to generate a neutral binuclear molecule (Figure 2). The four carboxylic protons are directed outwards and

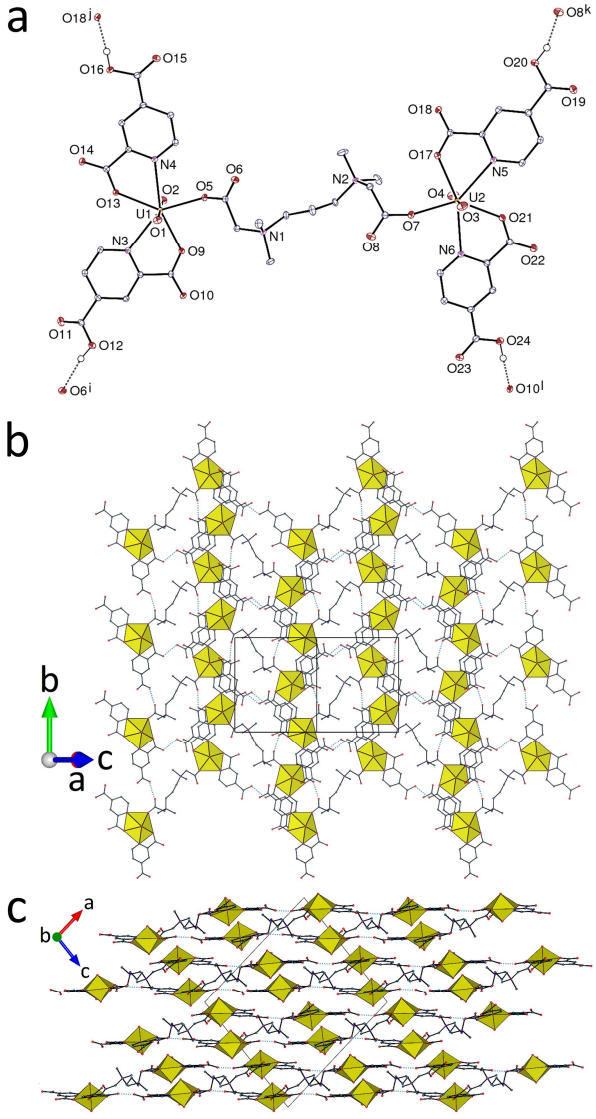

Figure 2. (a) View of compound **2**. Displacement ellipsoids are drawn at the 50% probability level. Carbon-bound hydrogen atoms are omitted and the hydrogen bonds are shown as dashed lines. Symmetry codes: i = x, y + 1, z; j = 2 – x, y + 1/2, 3/2 – z; k = x, y – 1, z; l = 1 – x, y – 1/2, 1/2 – z. (b) View of one double layer of hydrogen bonded molecules. Hydrogen bonds are shown as light-blue, dotted lines. (c) Packing with double layers viewed edge-on.

they are involved in hydrogen bonding to uncoordinated carboxylate oxygen atoms from four neighbouring molecules, with O12 and O20 associated as donors to the L2 atoms O6 and O8, and O16 and O24 to the 2,4-pydcH$^-$ atoms O18 and O10, respectively [O···O distances, 2.575(2)–2.678(2) Å; O–H···O angles, 160(3)–175(3)°]. These hydrogen bonds give rise to the formation of double layers parallel to (10$\bar{1}$) with tile-like overlapping molecules spanning the whole thickness of the sheets, the zwitterion units being located inside. The compact packing (KPI, 0.74) also entails multiple other interactions, among which the more prominent are parallel-displaced π-stacking interactions [centroid···centroid distances, 3.8914(11) and 4.0508(11) Å; dihedral angles, 9.51(9) and 12.63(9)°] and O(carboxylic/ate)···π interactions [O···centroid distances, 3.1657(19)–3.4469(17) Å].

Monoperiodic coordination polymers. The combination of isophthalic acid and the zwitterion L1 precursor provides a species, $[(UO_2)_2(L1)(ipht)_2]\cdot 4H_2O$ (**3**), where the full coordinative capacities of both ligands resulting from full deprotonation are similarly exploited in their action as bis($\kappa^2 O,O'$)-chelate bridges. The uranium atom is tris-chelated by two carboxylate groups from two ipht^{2-} ligands and one from the centrosymmetric L1 ligand and it is thus a 3-coordinated (3-c) node, while the ligands are simple links (Figure 3). The resulting monoperiodic coordination polymer is a double-stranded, ladder-like chain, albeit with sinuous rungs. The U^{VI} centres here are all in hexagonal-bipyramidal coordination, a situation which is commonly associated with diperiodic, approximately planar honeycomb structures but the conformation adopted by L1 is such that the two attached, parallel UO_6 (equatorial) units are not coplanar, which may explain why a more extended form of the polymer is not adopted. The flexible nature of L1 means that in principle it could add an aspect of chirality to the structure but the conformation adopted here is in fact centrosymmetric, as is that of the tetra-uranacyclic rings which fuse together to make the polymer. Each water molecule forms three hydrogen

bonds with carboxylate oxygen atoms as acceptors [O···O distances, 2.876(5)–3.147(5) Å; O–H···O angles, 121(4)–168(5)°], with that containing O10 in particular being involved in a bifurcated bond making a ring involving two oxygen atoms bound to the same metal centre, with the graph set descriptor[55,56] $R_1^2(4)$. As might be expected, there is stacking of the isophthalate rings [centroid···centroid distance, 3.584(2) Å; dihedral angle, 0°], apparent in the view down [100]. Double layers parallel to (010) are thus formed through side-by-side interlocking of polymer strands, giving a compact packing (KPI, 0.74).

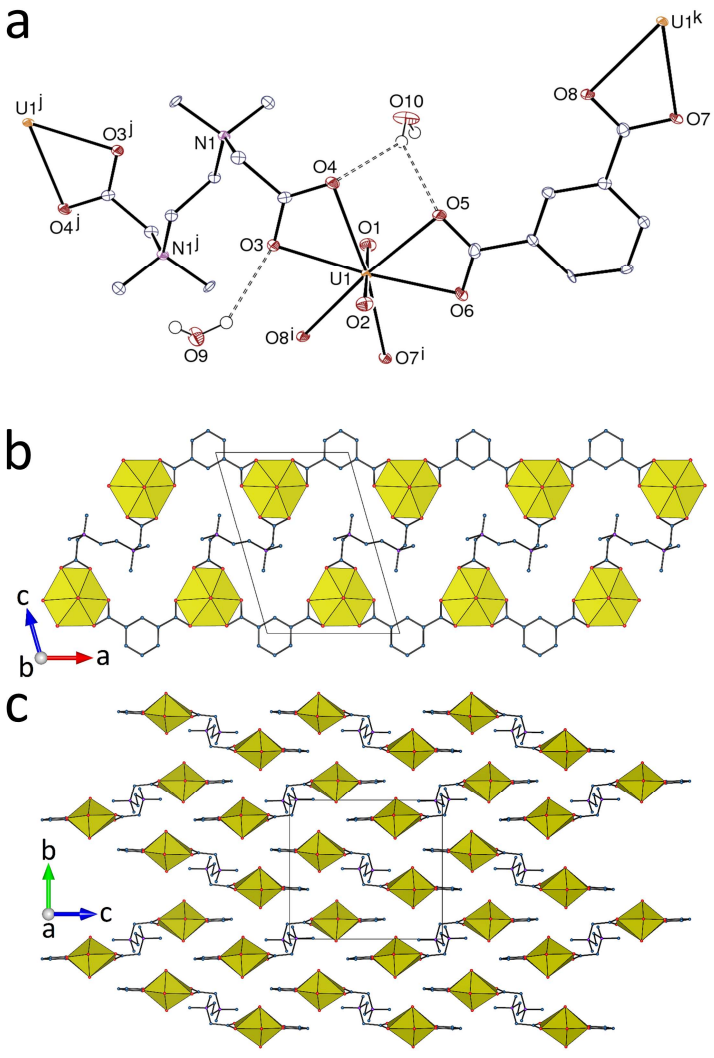

Figure 3. (a) View of compound **3**. Displacement ellipsoids are drawn at the 50% probability level. Carbon-bound hydrogen atoms are omitted and the hydrogen bonds are shown as dashed lines. Symmetry codes: i = $x + 1, y, z$; j = $2 - x, 1 - y, 1 - z$; k = $x - 1, y, z$. (b) View of one chain. (c) Packing with chains viewed end-on.

A complex with the same stoichiometry but a different connectivity, $[(UO_2)_2(L1)(pda)_2]$ (**4**), crystallizes from the mixture of 1,4-phenylenediacetic acid and the zwitterion L1 (Figure 4). The uranium atom is here κ^2O,O'-chelated by only one carboxylate group from pda^{2-}, the

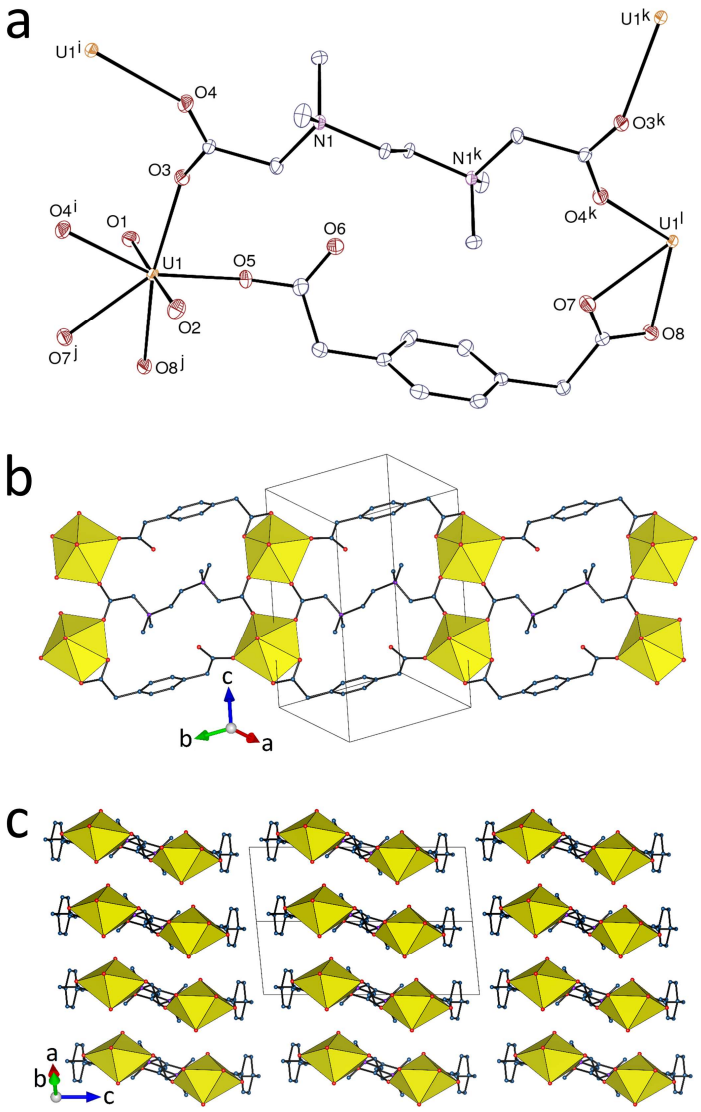

Figure 4. (a) View of compound **4**. Displacement ellipsoids are drawn at the 50% probability level and hydrogen atoms are omitted. Symmetry codes: i = –*x*, 2 – *y*, 1 – *z*; j = *x* – 1, *y* + 1, *z*; k = 1 – *x*, 1 – *y*, 1 – *z*; l = *x* + 1, *y* – 1, *z*. (b) View of one chain. (c) Packing with chains viewed end-on.

other group of the anion being monodentate, and the centrosymmetric zwitterion binds as a quadruply-bridging μ_4-bis(κ^1O:κ^1O') ligand, the metal centre being now in pentagonal-bipyramidal coordination. Uranium and L1 are thus 4-c nodes, while pda^{2-} is a simple link in

the double-stranded, monoperiodic polymer formed, which runs parallel to [1$\bar{1}$0]. The lateral rows formed by pda^{2-} links are analogous to those in **3**, but the central L1 ligands are oriented along the chain axis and dimers of doubly bridged uranyl ions are formed. The polymer strands lie side-by-side in a sheet parallel to (110) in such a way that phenyl rings are in close facial proximity [centroid···centroid distance, 4.1594(18) Å; dihedral angle, 0°], but with a large slippage of 1.95 Å. These interactions appear as purely dispersive from examination of the HS, and only the hydrogen atoms of the methyl groups and methylene bridges of L1 appear to be involved in intersheet CH···O interactions exceeding dispersion. The packing has a KPI of 0.72 and shows no solvent-accessible voids.

Diperiodic coordination polymers. The well-known capacity of the oxalate anion to block four equatorial sites of pentagonal-bipyramidal uranyl ions[57] is exhibited in the structure of $[(UO_2)_2(L1)(ox)_2]$ (**5**), where two oxalate anions chelate the metal centre and the centrosymmetric zwitterion L1 is restricted to a bis(κ^1O) bridging role (Figure 5). All ligands are edges and the uranium atom is a 3-c node in the diperiodic network formed, which is parallel to (1$\bar{1}$2) and has the common $\{6^3\}$ point symbol and **hcb** topological type. Rows of oxalate-bridged uranyl ions are linked by L1 molecules, which is as known for another zwitterionic ligand attached to the same polymer chain.[45] The packing of the puckered sheets involves slight interdigitation of the zwitterion units reflecting multiple CH···O interactions of the methyl groups and methylene bridges (KPI, 0.72). Oxalate ion has a special importance in actinide chemistry in general[58] and the polymer chain here is somewhat familiar but, as noted previously, it was not our actual intent to explore this chemistry further presently. The fact that the deposition of **5** required one of the longest reaction periods of the present series possibly indicates that any *cis*-muconate or 4-ketopimelate complexes were relatively soluble, favouring their slow consumption to leave only oxalate in solution.

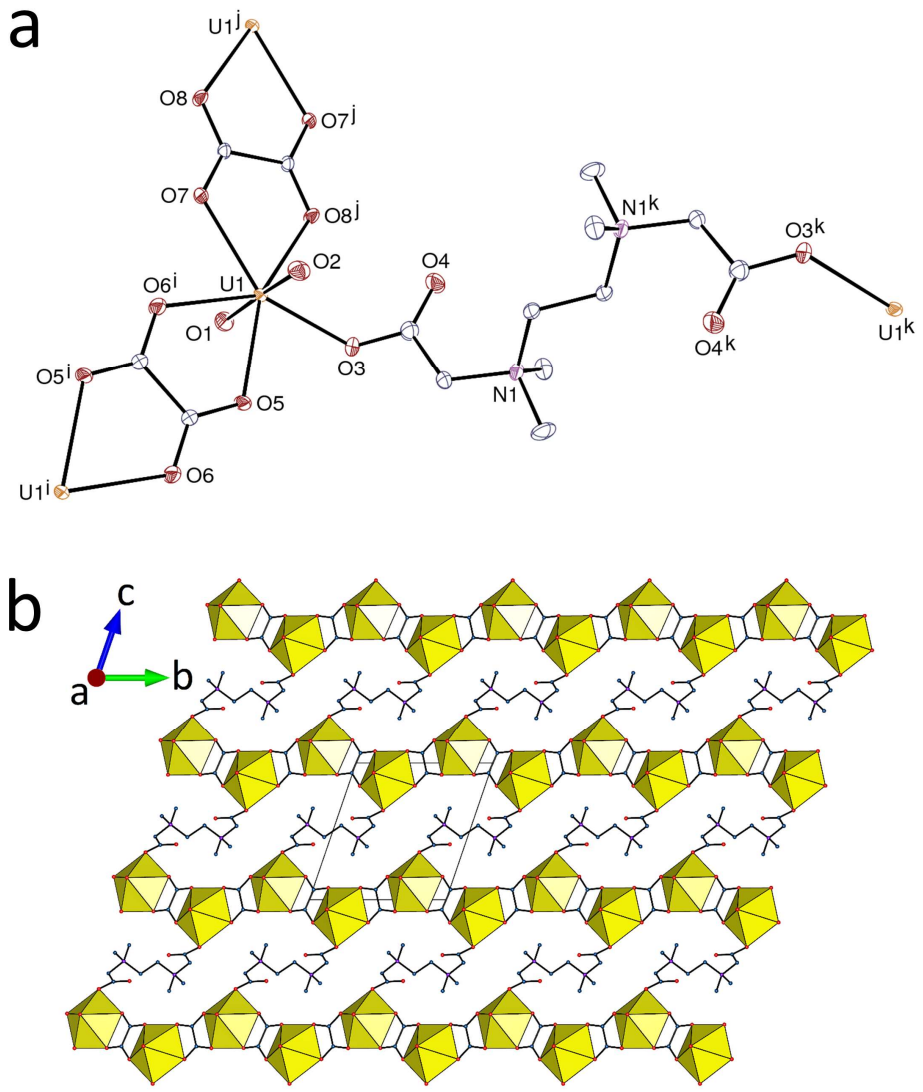

Figure 5. (a) View of compound **5**. Displacement ellipsoids are drawn at the 50% probability level and hydrogen atoms are omitted. Symmetry codes: i = 1 – *x*, 1 – *y*, –*z*; j = 2 – *x*, 2 – *y*, –*z*; k = –*x*, 2 – *y*, 1 – *z*. (b) Oblique view of the diperiodic assembly.

Compound **6**, $[(UO_2)_2(L2)(ipht)_2]\cdot H_2O$, provides the second example of crystallization of a complex of the more flexible zwitterion L2. As in compound **2**, the zwitterion binds as a bis(κ^1O) bridge between uranyl ions in a conformation lacking symmetry but with a divergent spatial disposition of the two carboxylate groups very similar to that seen for L1 (Figure 6). Its two coligands $ipht^{2-}$ also bridge uranyl centres but in a different manner to that in **3**, with one carboxylate acting as a κ^2O,O'-chelate and the other as a μ_2-κ^1O:κ^1O'-bridge, thus linking three

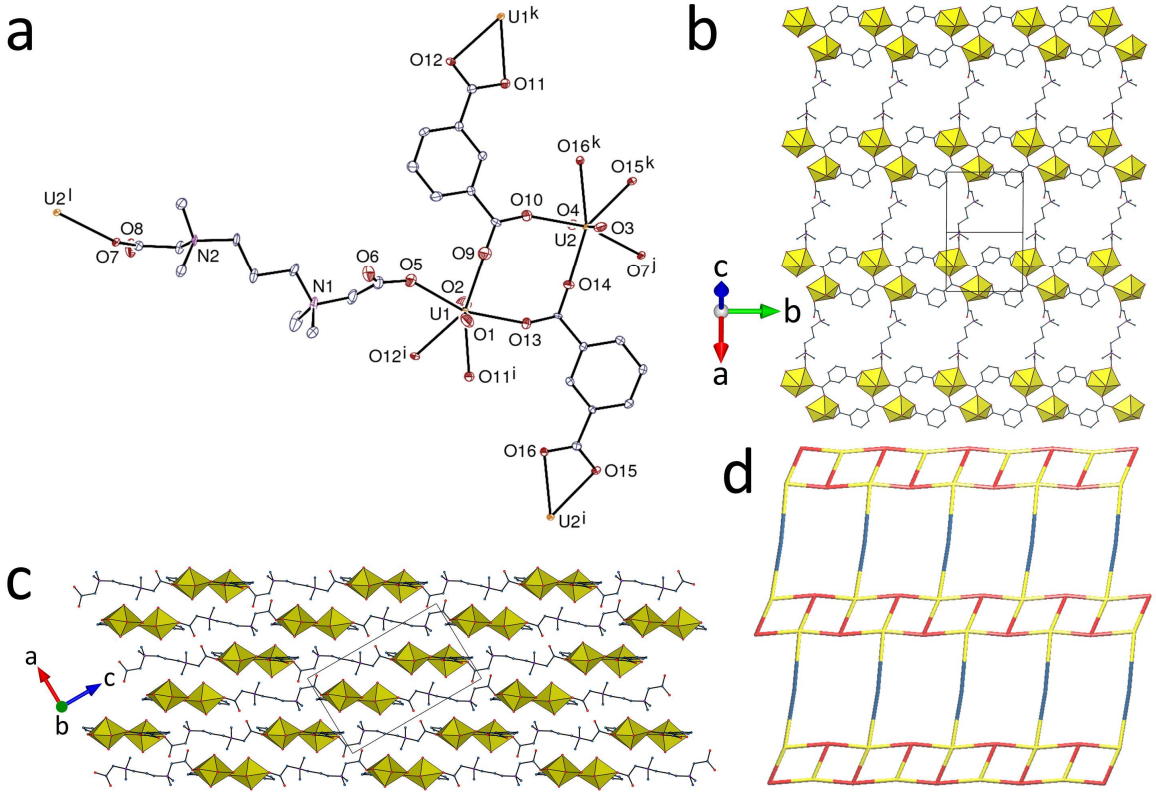

Figure 6. (a) View of compound **6**. Displacement ellipsoids are drawn at the 50% probability level and hydrogen atoms are omitted. Symmetry codes: i = *x*, *y* + 1, *z*; j = *x* – 1, *y*, *z* + 1; k = *x*, *y* – 1, *z*; l = *x* + 1, *y*, *z* – 1. (b) View of the diperiodic assembly. (c) Packing with layers viewed edge-on. (d) Nodal representation of the diperiodic network (uranium nodes, yellow; $ipht^{2-}$ nodes, red; L2 edges, blue; same orientation as in (b)).

uranyl ions. The two uranium centres, in similar environments, are thus 4-c nodes, the $ipht^{2-}$ anions are 3-c nodes and L2 is a simple edge in the 2-nodal diperiodic network parallel to (101), which has the $\{4^2.6^3.8\}\{4^2.6\}$ point symbol and the V_2O_5 topological type. This arrangement is similar to that found in a uranyl ion complex with *cis/trans*-1,3-cyclohexanedicarboxylate and a bis(carboxylatopyridinium)-based zwitterionic ligand.[16] No π-stacking interaction is present here, all centroid···centroid distances being larger than 4.58 Å, but a CH···π interaction involving a proton from L2 may be present [H···centroid distance, 2.84 Å; C–H···centroid angle, 169°]. Once again, the dominant intersheet contacts involve multiple CH···O interactions of the aliphatic components of the zwitterion. The KPI is only 0.64, some voids in the structure containing unresolved solvent molecules (see Experimental Section).

Use of a third pyridinedicarboxylic acid isomer, the 2,5 form, along with the L1 precursor provided compound $[(UO_2)_2(L1)(2,5\text{-pydc})_2]\cdot 4H_2O$ (**7**), shown in Figure 7. The unique uranium atom is chelated in the N,O site of one 2,5-pydc^{2-} ligand, and κ^2O,O'-chelated

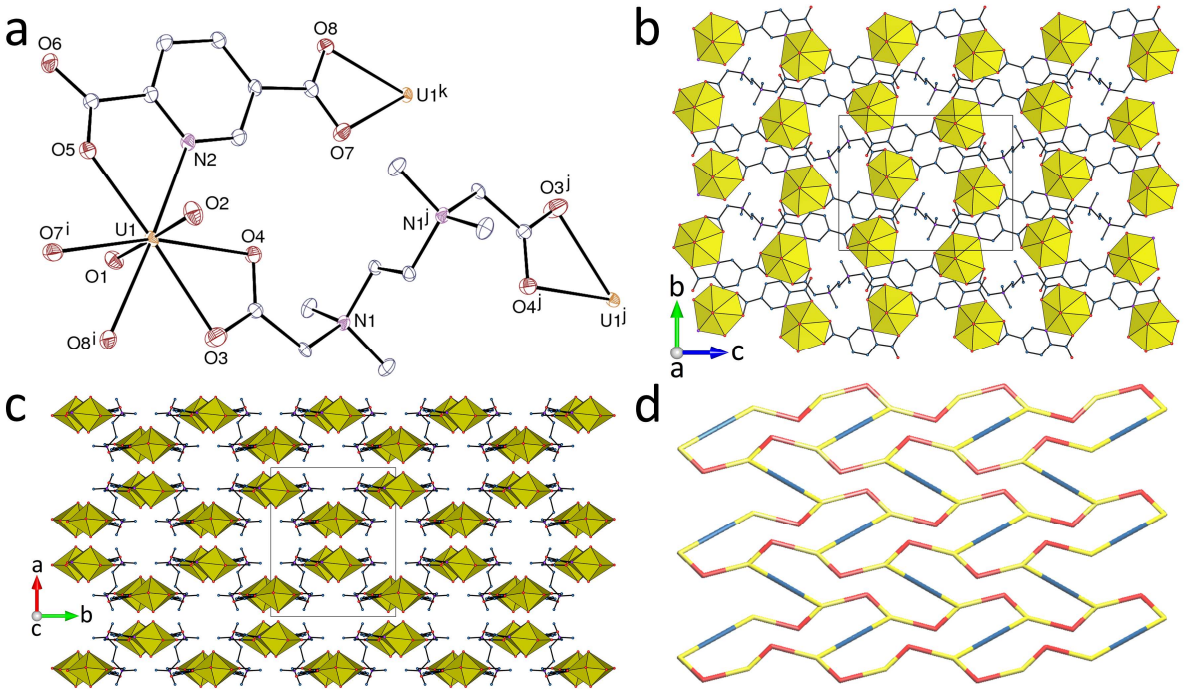

Figure 7. (a) View of compound **7**. Displacement ellipsoids are drawn at the 50% probability level and hydrogen atoms are omitted. Symmetry codes: i = *x*, 1 – *y*, *z* – 1/2; j = 3/2 – *x*, 3/2 – *y*, 1 – *z*; k = *x*, 1 – *y*, *z* + 1/2. (b) View of the **hcb** diperiodic assembly. (c) Packing with layers viewed edge-on. (d) Nodal representation of the diperiodic network (uranium nodes, yellow; 2,5-pydc^{2-} edges, red; L1 edges, blue; same orientation as in (b)).

by the other carboxylate group in a second 2,5-pydc^{2-} ligand and by the centrosymmetric L1. N,O-chelation by 2,5-pydc^{2-} is observed in all the uranyl ion complexes with this ligand reported so far, the distal carboxylate group being either monodentate or μ_2-κ^1O:κ^1O'-bridging.[59–62] Uranium in **7** is thus a 3-c node and both ligands are simple edges, the diperiodic network formed, parallel to (100), having here also the **hcb** topology, with very distorted cells. Viewed down [001], the sheets display a square-wave shaped section and they can be described as bilayers with faces consisting of side-by-side strands of $[UO_2(2,5\text{-pydc})]_n$ polymer which are linked to strands in the other face by bridging L1 molecules, thus placing the aliphatic

components within the double layer. The packing is of the bump-to-bump type, thus defining small channels directed along [001] and containing the water molecules which, although not all protons were found, probably connect different layers through hydrogen bonding (KPI, 0.74). This does not lead, however, to any obvious favouring of aromatic-aromatic interactions between layers, all centroid···centroid distances being larger than 4.9 Å.

Determination of the crystal structure of $[(UO_2)_2(L1)(dnhpa)_2]$ (**8**), obtained from the reaction mixture containing 1,2-phenylenedioxydiacetic acid and L1 showed the diacid to have undergone a fairly radical conversion into a dinitrophenoxide derivative, 3,5-dinitro-2-hydroxyphenoxyacetic acid ($dnhpaH_2$). Given that uranyl ion complexes of the intact diacid dianion can be isolated under similar solvothermal conditions,[63,64] albeit in low yields and, possibly significantly, sometimes involving *in situ* production of oxalate,[64] a possible explanation of this difference is the presence of chloride anion introduced with $L1H_2Cl_2$. Halide-assisted dealkylation of ethers is a well-known procedure involving activation by Lewis acids such as B^{III} and Al^{III},[65] so that chloride attack on an ether activated by coordination to U^{VI} seems plausible, at least under solvothermal conditions. Removal of one carboxymethyl group from 1,2-phenylenedioxydiacetic acid would generate a substituted phenol and phenols in general are known to undergo facile nitration even in dilute nitric acid.[66] Although we have not checked to see if compound **8** is explosive (like other nitro-aromatics), our assessment of the chemistry here indicates that there may well be occasions when the use of uranyl nitrate as a source of U^{VI} for solvothermal syntheses should be avoided. Quite apart from any issues of safety, the implication of this anion effect is that efforts to restrict the anion present in the reaction media to a single species such as triflate might result in product differences in some cases. The unique uranium atom in **8** is chelated in the O_3 site of the $dnhpa^{2-}$ ligand, containing carboxylate, hydroxide and ether donors, and is bound to one more carboxylate group from a second $dnhpa^{2-}$ ligand, the carboxylate being μ_2-κ^1O:κ^1O'-bridging, and one monodentate

carboxylate of the centrosymmetric L1 molecule (Figure 8). Here also, the metal centre is a 3-c node and both ligands are edges in the **hcb** network formed, parallel to (001). As in **7**, the sheets are heavily corrugated, with the zwitterion units defining a gently undulating central

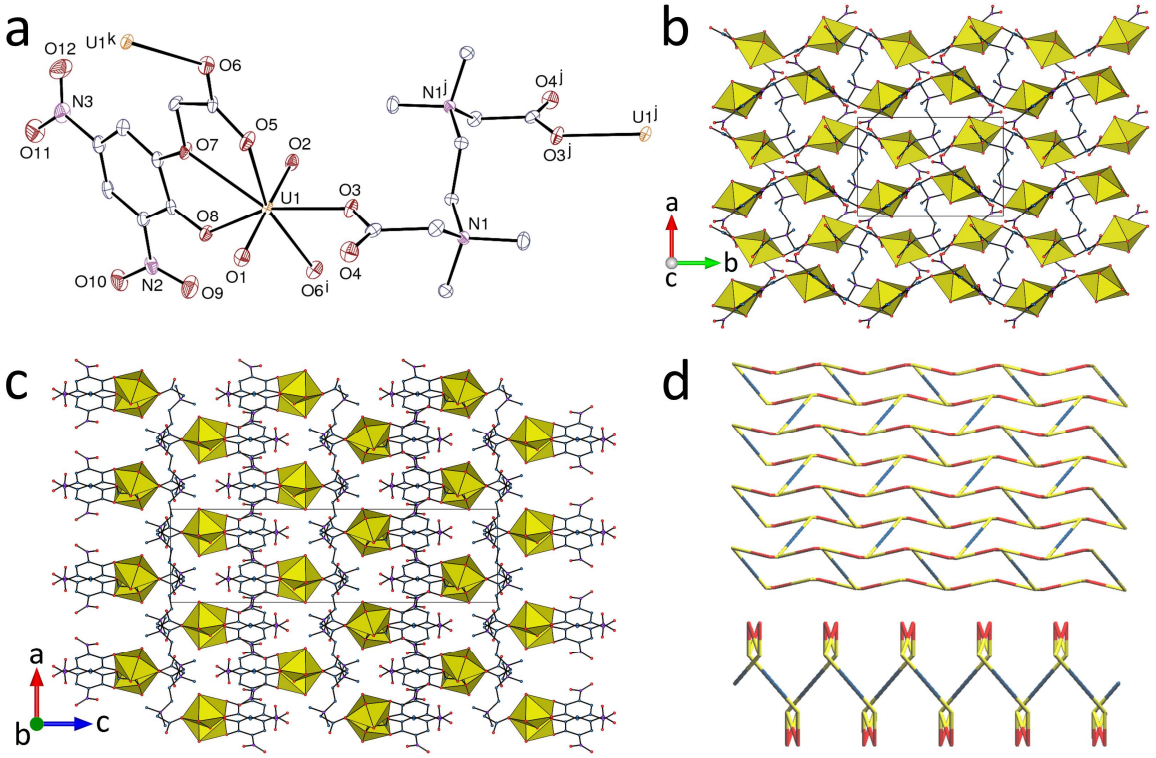

Figure 8. (a) View of compound **8**. Displacement ellipsoids are drawn at the 50% probability level and hydrogen atoms are omitted. Symmetry codes: i = 3/2 – *x*, *y* + 1/2, *z*; j = 2 – *x*, 1 – *y*, 1 – *z*; k = 3/2 – *x*, *y* – 1/2, *z*. (b) View of the **hcb** diperiodic assembly. (c) Packing with layers viewed edge-on. (d) Two views of the nodal representation of the diperiodic network, down [001] (top) or [010] (bottom) (uranium nodes, yellow; dnhpa^{2-} edges, red; L1 edges, blue).

sheet from which uranyl ions and dnhpa^{2-} project to either side and interdigitate with those of adjacent sheets (KPI, 0.74). This interdigitation creates parallel arrays (stacks) of aromatic units but, as is well known for nitroaromatics,[67] ones where the nitro groups take an important part in the interactions. No π-stacking interaction is apparent here; the nitro atom O10 points toward an aromatic ring [O···centroid distance, 3.199(3) Å; N–O···centroid angle, 88.9(2)°] but, although it is apparent on the HS, this interaction is not prominent, the most notable interactions

of the nitro groups being hydrogen bonds involving methylene protons of both $dnhpa^{2-}$ and L1.

The tetracarboxylic acid combined with $L1H_2Cl_2$ for the synthesis of complex $[(UO_2)_3(L1)(thftcH)_2(H_2O)]$ (**9**), tetrahydrofurantetracarboxylic acid, $thftcH_4$, is commercially available as its achiral 2*R**,3*R**,4*S**,5*S** diastereomer but is known in some cases under solvothermal conditions to provide complexes of its deprotonated chiral 2*R**,3*R**,4*R**,5*S** form,[68,69] for which reason it has even been suggested that it might be considered as a single-molecule dynamic covalent library. In compound **9**, however, it appears to show the more typical behaviour of retention of configuration, although disorder of the $thftcH^{3-}$ ring does create some uncertainty as to the configuration of the ill-resolved minor component. The asymmetric unit contains two inequivalent uranyl ions, one of them (U1) being bound to two carboxylate groups of one $thftcH^{3-}$ anion (seven-membered chelate ring), two more carboxylate donors from another $thftcH^{3-}$ and L1, and a water molecule, and the other (U2), located on an inversion centre, being twice chelated in the O_3 site of two $thftcH^{3-}$ ligands (Figure 9). The versatility of deprotonated $thftcH_4$ as a ligand is seen here in its action as a bidentate chelate on one U^{VI} centre, a tridentate chelate on a second, and a monodentate donor on a third. In contrast, L1 displays its relative lack of versatility in maintaining the same centrosymmetric conformation as seen in several previous instances. Although L1 is still a simple edge in the diperiodic polymer formed, as well as U2, U1 and $thftcH^{3-}$ are 3-c nodes. The uninodal network is parallel to (101) and it has the point symbol $\{4.8^2\}$ and the common **fes** topological type. The thick layers can be seen as built up from monoperiodic strands, in which $thftcH^{3-}$ ligands link in alternation binuclear pentagonal-bipyramidal uranyl units and mononuclear hexagonal-bipyramidal uranyl units, being cross-linked by L1, which is now becoming a common pattern. The cross-linking here is assisted by the formation of hydrogen bond "dimer" units involving the undeprotonated carboxylic groups of two $thftcH^{3-}$ anions [O10···O11^{i}, 2.576(9) Å; O10–H10···O11^{i}, 169(11)°; symmetry code: i = 1 – *x*, –*y*, 2 – *z*]. The coordinated water molecule

forms hydrogen bonds both within and between sheets with oxo and carboxylato oxygen acceptors [O···O distances, 2.737(8)–2.991(8) Å; O–H···O angles, 127.(7)–173.(8)°], and CH···O interactions of the methyl groups and methylene bridges of L1 further reinforce intersheet connection, the packing being quite compact (KPI, 0.75).

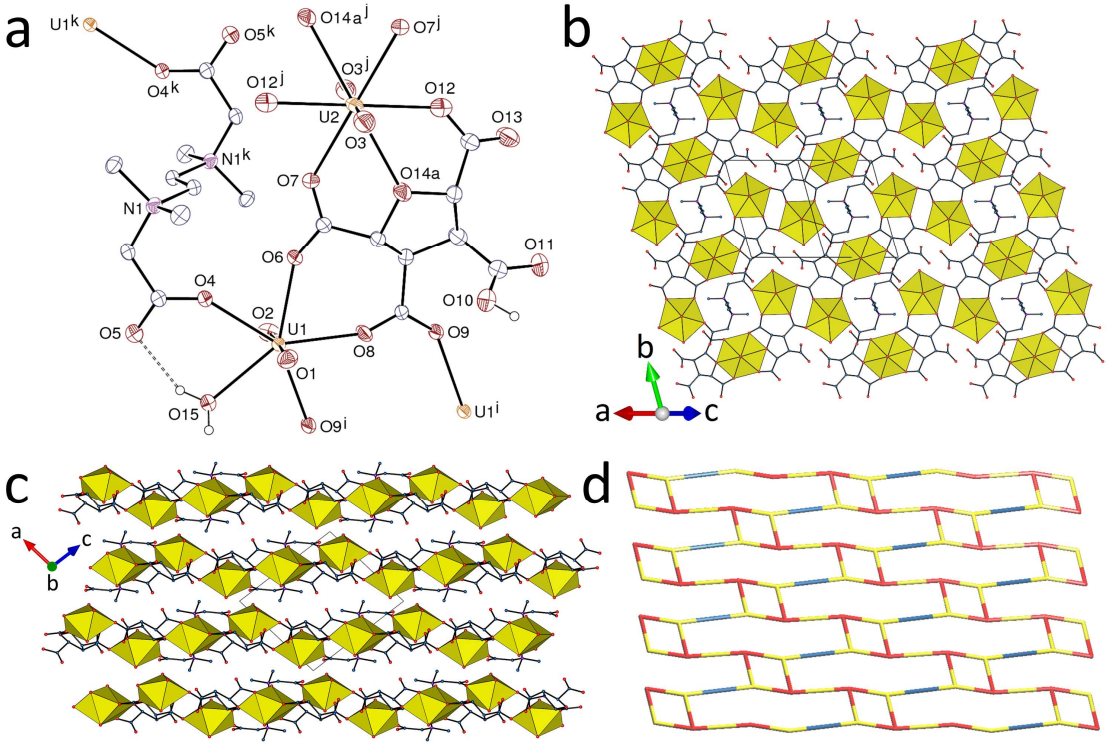

Figure 9. (a) View of compound **9**. Displacement ellipsoids are drawn at the 30% probability level. Carbon-bound hydrogen atoms are omitted and the hydrogen bond is shown as a dashed line. Only one position of the disordered atoms is represented. Symmetry codes: i = 1 – *x*, 1 – *y*, 2 – *z*; j = 2 – *x*, –*y*, 1 – *z*; k = 2 – *x*, 1 – *y*, 1 – *z*. (b) View of the **fes** diperiodic assembly. (c) Packing with layers viewed edge-on. (d) Nodal representation of the diperiodic network (uranium nodes, yellow; $thftcH^{3-}$ nodes, red; L1 edges, blue; view down [101] with [010] vertical).

The nature of the complex $[(UO_2)_2Cl_2(L1)_3][(UO_2Cl_3)_2(L1)]$ (**10**) is somewhat remarkable given that terephthalate is well established as a good ligand for U^{VI}, with about 40 crystal structures reported in the CSD, yet it is not incorporated in this product while the dizwitterion is. There are other remarkable aspects, firstly in that it is an ionic species,

consisting of binuclear, zwitterion-bridged $[(UO_2Cl_3)_2(L1)]^{2-}$ anions associated with the $[(UO_2)_2Cl_2(L1)_3]^{2+}$ cationic coordination polymer (Figure 10). In the centrosymmetric anion,

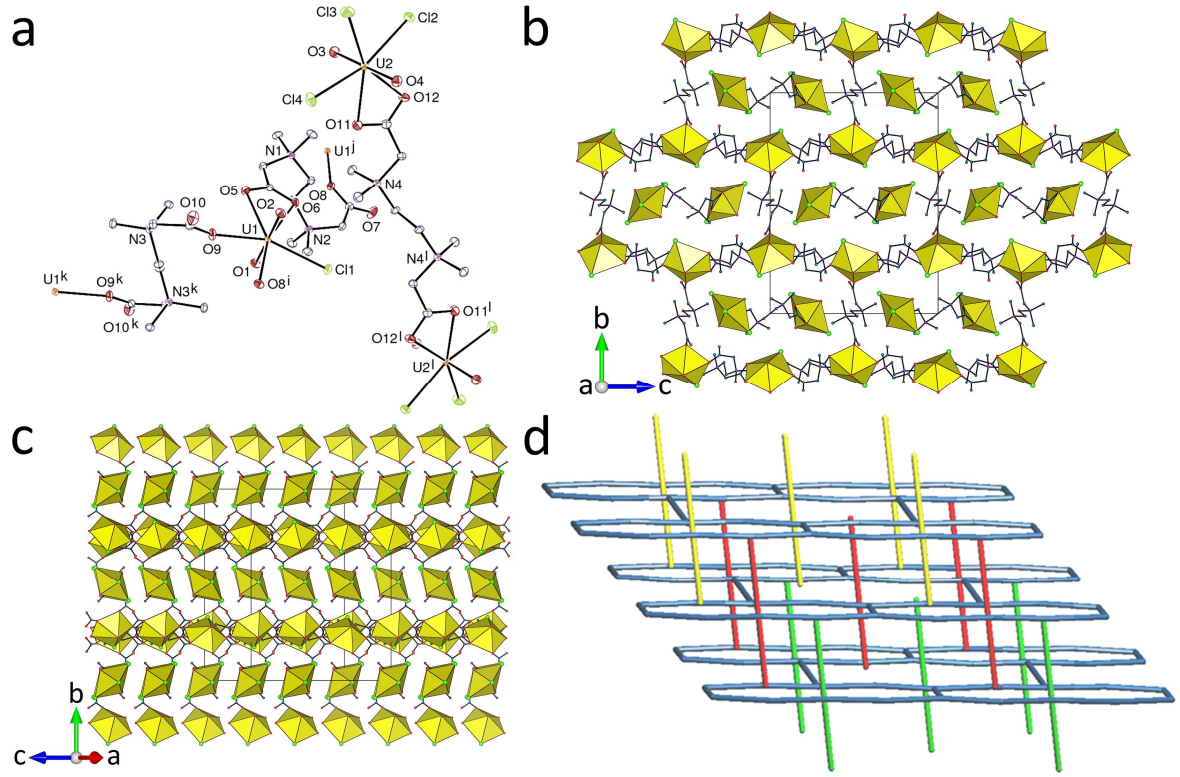

Figure 10. (a) View of compound **10**. Displacement ellipsoids are drawn at the 50% probability level and hydrogen atoms are omitted. Symmetry codes: i = x + 1/2, 1/2 – y, z – 1/2; j = x – 1/2, 1/2 – y, z + 1/2; k = 1 – x, –y, 1 – z; l = 1 – x, 1 – y, 1 – z. (b) View of the cationic **hcb** diperiodic assembly with the included dinuclear anions. (c) Packing with layers viewed side-on. (d) Simplified view showing three layers with the anions included in each of different colors.

the uranium atom is κ^2O,O'-chelated by L1 and bound to three terminal chloride anions whereas, in the cation, it is κ^2O,O'-chelated by one L1 ligand, and bound in monodentate fashion to two other L1 molecules and to one chloride anion. One of the L1 ligands in the cation has no symmetry but is pseudo-centrosymmetric, and it is bound in the bridging μ_2-($\kappa^2O,O';\kappa^1O''$) mode, and the other is centrosymmetric and bound in the μ_2-bis(κ^1O) mode. U1 is thus a 3-c node and both L1 molecules are edges, which gives the usual **hcb** network, parallel here to (101). However, an unusual feature is that each hexanuclear ring is perforated by one

rod-like anion, with two more, associated to the next layer on each side, having their head level with the ring (Figure 10d). This 0D + 2D arrangement involving linear discrete components can be seen as a close approach to 1D + 2D semi-interpenetration (in which the components are ideally separable without bond breakage), as recently found in a complex with the $Ni(tpyc)_2$ zwitterion and the citrate ligand.[15] These rods provide three-periodic connectivity, in particular through CH···Cl hydrogen bonds[70,71] involving all chloride anions except Cl4 [C···Cl distances, 3.491(3)–3.682(3) Å; H···Cl distances, 2.57–2.78 Å; C–H···Cl angles, 131–161°]. Although weak, these interactions are multiple and more numerous than the usual CH···O hydrogen bonds, with Cl2 being involved in four bonds, and Cl1 and Cl3 in two. The packing does not show any solvent-accessible space (KPI, 0.72). That the cationic polymer incorporating just the zwitterion has cavities able to accommodate quite large species is interesting but it remains to be seen just how stable a solid state entity this may be.

Triperiodic frameworks. As, in our experience, has quite often been the case with 2,5-thiophenedicarboxylate,[15,72] this is a ligand which can provide surprises. In the ionic compound $[(UO_2)_5(L1)_7(tdc)(H_2O)][(UO_2)_2(tdc)_3]_4{\cdot}CH_3CN{\cdot}12H_2O$ (**11**), there is almost complete "self sorting" of the tdc^{2-} and L1 ligands, with the anions involving exclusively the former and the cations a 7:1 L1:tdc^{2-} mixture. There are seven uranyl cations and seven tdc^{2-} ligands (one of each with twofold rotation symmetry), and four inequivalent L1 units (one with inversion symmetry) in the asymmetric unit. The cationic part, $[(UO_2)_5(L1)_7(tdc)(H_2O)]^{8+}$, contains three of the inequivalent uranium atoms, all in different environments. U1, located on a twofold rotation axis, is bound to four carboxylate donors from four L1 molecules and to one water molecule, U2 is bound to three carboxylate donors from three L1 molecules and one κ^2O,O'-chelating tdc^{2-} ligand, and U3 is κ^2O,O'-chelated by three L1 molecules (Figure 11). The four inequivalent L1 molecules are bound in the μ_3-($\kappa^2O,O';\kappa^1O'':\kappa^1O'''$), μ_2-bis(κ^1O), μ_2-($\kappa^2O,O';\kappa^1O''$), and μ_2-bis(κ^2O,O') modes, tdc^{2-} being also bound in the latter mode. Of these

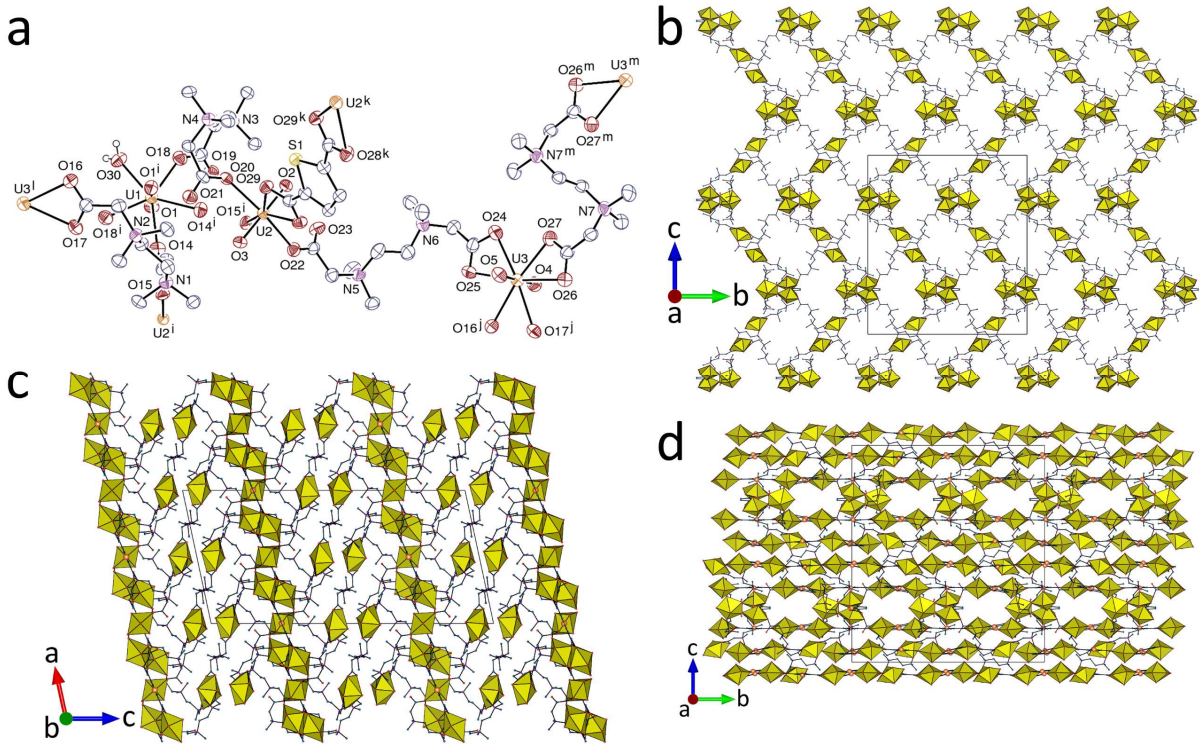

Figure 11. (a) View of the cationic part of compound **11**. Displacement ellipsoids are drawn at the 50% probability level and carbon-bound hydrogen atoms are omitted. Symmetry codes: i = –*x*, *y*, 1/2 – *z*; j = 1/2 – *x*, *y* + 1/2, 1/2 – *z*; k = 1 – *x*, *y*, 1/2 – *z*; l = 1/2 – *x*, *y* – 1/2, 1/2 – *z*; m = 3/2 – *x*, 3/2 – *y*, 1 – *z*. (b) and (c) Two views of the triperiodic framework alone. (d) View of the complete, hetero-entangled structure.

four inequivalent L1 units, two have a conformation close to that observed in all the other L1-containing species described herein but two are finally seen to adopt a conformation which is chiral and C-shaped, showing that conformational barriers within the zwitterion can be overcome. Overall, U1 and U2 are 4-c nodes, U3 is a 3-c node and all ligands are simple edges except for one L1 which is also a 3-c node. A 4-nodal, triperiodic framework is thus generated, which has the point symbol $\{3.7.8.9.11^2\}_2\{3.7.8\}_2\{3^2.7.8^2.9\}\{7.8^2\}_2$ and is shown in Figure 12a. Two different kinds of channels with very irregular cross-sections of about 8–10 Å in width appear to run along [100]. Considering now the anionic part, four of the inequivalent U^{VI} sites and six of the inequivalent tdc^{2-} ligands, all bis(κ^2O,O')-chelating, are found within two inequivalent (but very similar), nearly planar diperiodic $[(UO_2)_2(tdc)_3]_n$ polymer units with **hcb**

topology and uranium atoms as 3-c nodes, a usual feature with this ligand.[72–76] The large size of the hexanuclear cells in the uranyl ion complexes with tdc^{2-} allows for frequent occurrences

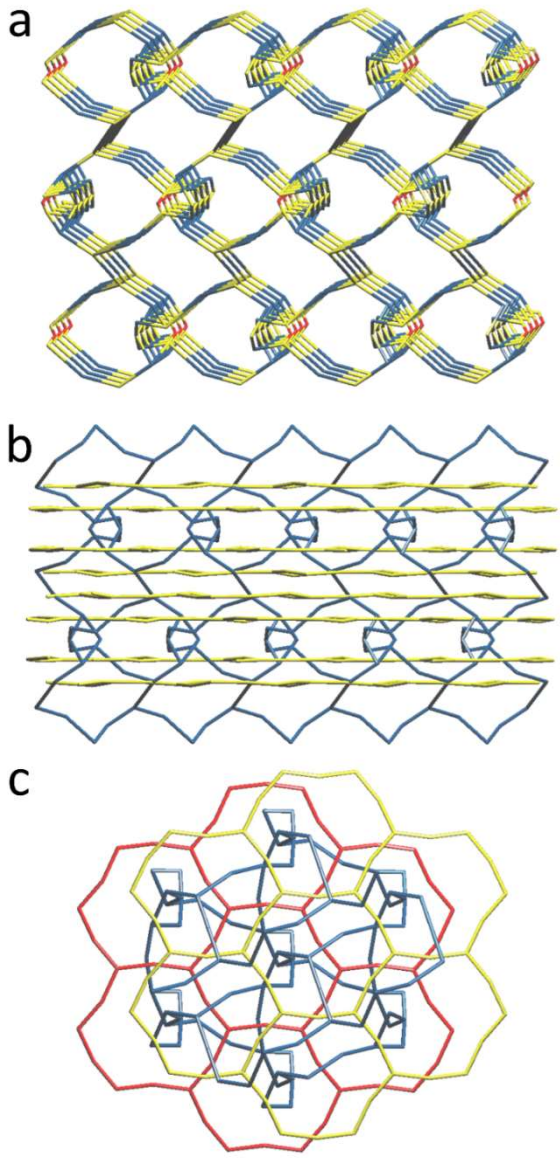

Figure 12. (a) Nodal representation of the triperiodic framework in **11** (uranium nodes, yellow; L1 nodes and edges, blue; tdc^{2-} edges, red; [010] horizontal, [001] vertical). (b) Simplified view of the hetero-entanglement with triperiodic framework in blue and **hcb** layers in yellow. (c) Simplified view showing two **hcb** layers in red and yellow and the entangled triperiodic framework in blue.

of interpenetration or polycatenation.[72,74–76] With nearly planar sheets as observed here, 2D + 2D → 3D inclined polycatenation has been found,[75] while undulated sheets are associated with 2- or 3-fold 2D + 2D parallel interpenetration.[72,74,76] However, a novel mode of association is

found here, the cationic framework and anionic layers being associated through 2D + 3D hetero-interpenetration, the two components having both different periodicities (hence topologies) and compositions[24–27] (Figure 12b,c). The inequivalence of the different anionic layers arises from differences in their environment; when viewed down [100], where the sheets are seen edge-on, they make groups of four closely packed with one another, with a larger separation between groups. The two equivalent outermost layers in one group occupy spaces in one of the channel types, and each of their hexanuclear cells is crossed by two L1 edges of the framework linked to atom U2 and it contains also part of the C-shaped ligand connecting U1 and U2; the two central layers are mainly associated with the other channel type and their cells contain atom U3, two edges bound to it directed on one side of the cell and the third on the other side. The water ligand is hydrogen bonded to an uncoordinated water molecule, but a more detailed examination of the hydrogen bond pattern is hampered by both the positions of the hydrogen atoms of the uncoordinated water molecules being unknown, and the presence of additional, unresolved solvent molecules (see Experimental Section), the KPI being 0.68. Two possibly significant parallel-displaced π-stacking interactions may be formed by thiophene rings pertaining either to the cation and one of the anions or to the two anions [centroid···centroid distances, 3.915(4) and 4.144(4) Å; dihedral angles, 7.7(3) and 14.7(3)°], but their contribution to the formation of the assembly is probably extremely minor at best, electrostatic interactions being dominant between the di- and triperiodic components.

The structure of $[(UO_2)_7(O)_3(OH)_{4.3}Cl_{2.7}(L2)_2]Cl\cdot 7H_2O$ (**12**) provides another example of where the ability of a dizwitterion to crosslink strands of a monoperiodic polymer leads to species of considerably greater potential interest, here one containing channels of significant size. The asymmetric unit contains four uranium atoms in slightly different environments: U1, U2 and U3 are bound to one chloride anion, one carboxylate donor, and three oxo/hydroxo anions (two oxo and one hydroxo for U1, and the reverse proportion for U2 and U3), while U4,

located on a twofold rotation axis, is bound to two carboxylate donors from two different L2 molecules, one oxo and two hydroxo anions (Figure 13). Ignoring the attachment of L2, the

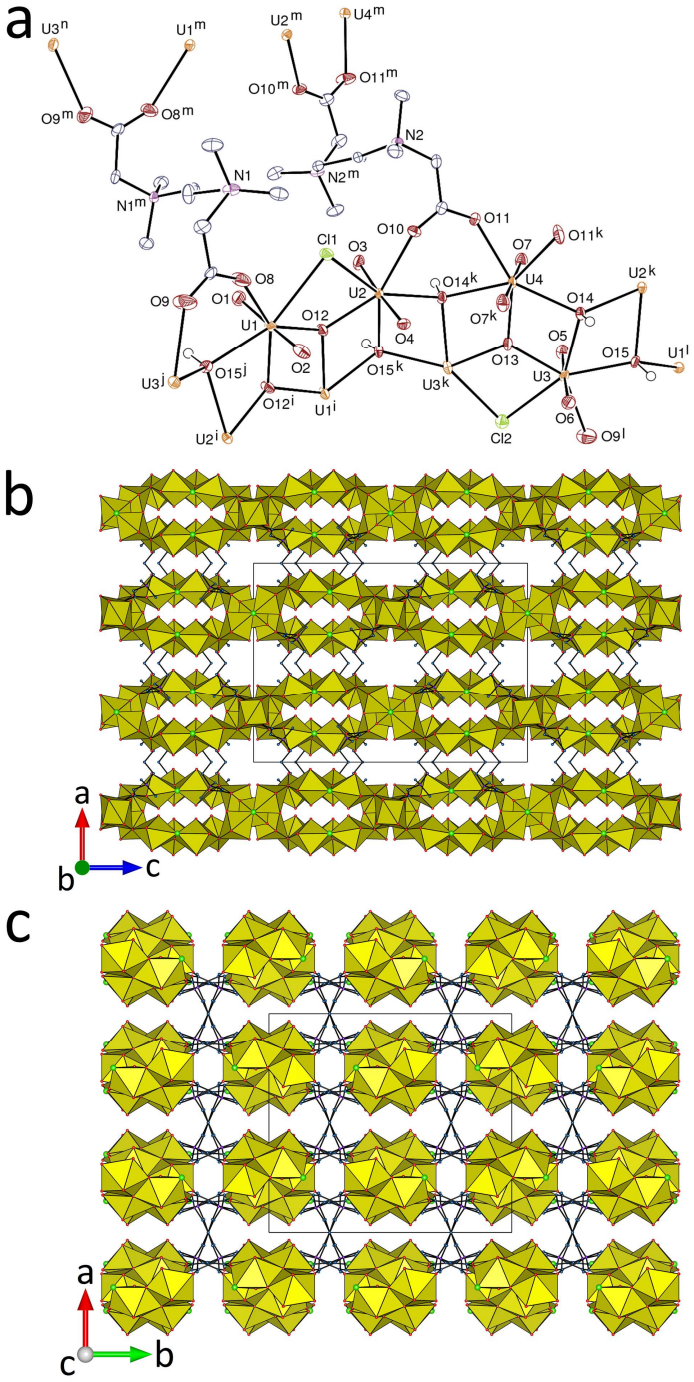

Figure 13. (a) View of compound **12**. Displacement ellipsoids are drawn at the 50% probability level and carbon-bound hydrogen atoms are omitted. The disordered hydroxide close to Cl2 is not shown. Symmetry codes: i = *x*, 1 – *y*, 1/2 – *z*; j = 3/2 – *x*, 1 – *y*, *z* – 1/2; k = 3/2 – *x*, *y*, 1 – *z*; l = 3/2 – *x*, 1 – *y*, *z* + 1/2; m = 2 – *x*, 3/2 – *y*, *z*; n = *x* + 1/2, *y* + 1/2, *z* – 1/2. (b) and (c) Two views of the interpenetrated triperiodic frameworks.

coordination polymer present is just an undulating, monoperiodic chlorouranate directed along [001], the presence of oxo and hydroxo bridges indicating that its formation may have occurred under more basic conditions than applied on the other syntheses described herein. In that the reaction mixture contained CsI, added in order for I_3^- to be formed by nitrate oxidation (as observed in related work[14]), its oxidation would have led to a consumption of acid and thus to conditions leading to uranyl ion hydrolysis, explaining what has been observed. Both L2 ligands have twofold rotation symmetry and they are bound in the μ_4-bis(κ^1O:κ^1O')-bridging mode previously found for L1 in **4**. They connect the chlorouranate chains so as to form a triperiodic framework possessing wide cavities since the undulating chains are packed in bump-to-bump fashion and linked to one another at their point of shorter contact (Figure 14a). The cavities are

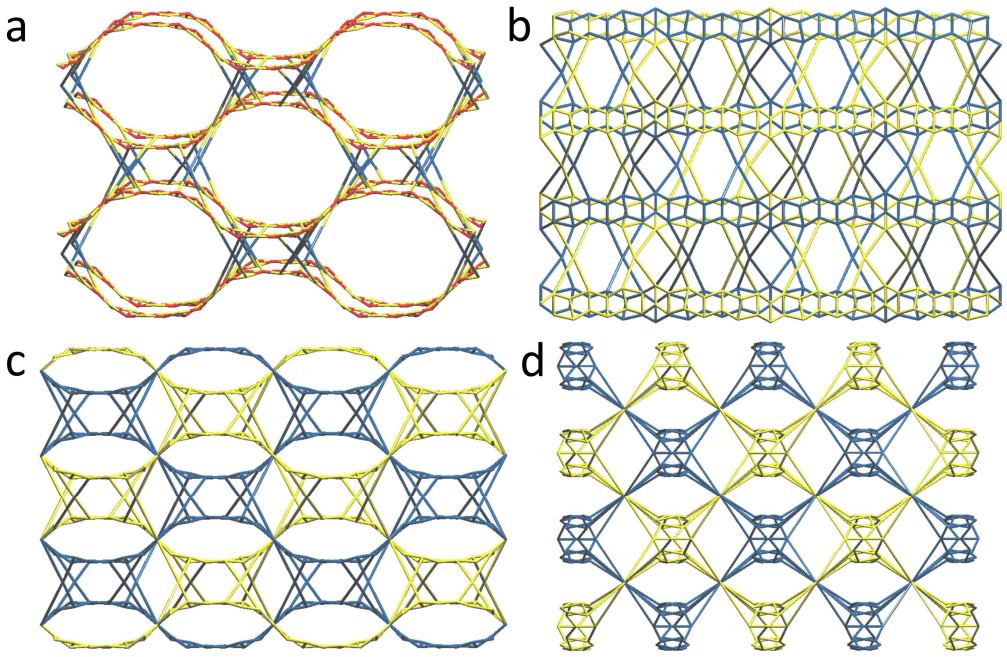

Figure 14. (a) Nodal representation of one triperiodic framework in **12** (uranium nodes, yellow; oxo/hydroxo nodes, red; L2 nodes, blue; [001] horizontal, [100] vertical, slightly rotated). Three views of the interpenetrated frameworks, down [100] with [010] vertical (b), down [010] with [100] vertical (c), and down [001] with [100] vertical (d). Chloride edges are omitted in all views for clarity.

sufficiently large for twofold interpenetration to occur (Figure 14b–d), with inversion as full interpenetration symmetry element (class IIa).[77] The hydroxide anions are hydrogen bond

donors to free water molecules, but further analysis of the hydrogen bond network is precluded by the disorder affecting some water molecules, and by the presence of additional, disordered water molecules which were not located (see Experimental Section), as shown by the KPI of ~0.68.

Discussion of the structures. The present results confirm the interest of using mixtures of zwitterionic and anionic polycarboxylates to generate mixed-ligand uranyl ion complexes spanning a very large range of topologies. Among the 12 complexes reported, whose structural characteristics are summarized in Table 3, only **1**, **10** and **12** do not include both kinds of ligands

Table 3. Overview of the Geometry of the Complexes

compound	zwitterion (L)	anion (A^{x-})	Connectivity[a]			periodicity	geometrical features
			U	L	A^{x-}		
1	L1	2,6-pydc^{2-}				0	mononuclear anionic complex
2	L2	2,4-pydcH^{-}	1	2		0	binuclear neutral complex
3	L1	ipht^{2-}	3	2	2	1	double-stranded chain
4	L1	pda^{2-}	4	4	2	1	double-stranded chain
5	L1	ox^{2-}	3	2	2	2	**hcb** network
6	L2	ipht^{2-}	4	2	3	2	V_2O_5 network
7	L1	2,5-pydc^{2-}	3	2	2	2	**hcb** network
8	L1	dnhpa^{2-}	3	2	2	2	**hcb** network
9	L1	thftcH^{3-}	2/3	2	3	2	**fes** network
10	L1	Cl^{-}	3	2[b]		0 + 2	**hcb** cationic network and binuclear anions
11	L1	tdc^{2-}	3/4	2/3	2	2 + 3	hetero-interpenetrated structure
12	L2	O^{2-}/OH^{-}/Cl^{-}	5	4	2/3	3	2-fold interpenetrated framework

[a] Terminal ligands are not taken into consideration. [b] Connectivity in the polymer only.

coordinated to uranyl. Uranyl is only bound to 2,6-pydc^{2-} in complex **1**, possibly due to the high stability and low solubility of the complex formed, while **10** and **12** involve only the zwitterionic carboxylate, associated with chlorido, oxo and hydroxo donors. In the case of **10** in particular, the presence of chloride in the reaction mixture is obviously important in regard to the product composition since it appears that CH···Cl interactions are dominant in the solid state cation-anion contacts, probably explaining the influence of chloride on product solubility;

the exclusion of terephthalate from the isolated complex is however unexpected considering that the related ligand isophthalate is coordinated in complexes **3** and **6**. Overall, the number of complexes involving L1 (9) is much larger than that with L2 (3), which genuinely reflects the more amenable character of the complexes of the former to crystallization, since the same attempts were performed with both. Compared with the zwitterionic dicarboxylates previously used in similar studies,[14–17] enhanced flexibility could be expected from L1 and L2, and indeed several conformations have been found for both ligands. Three main geometries are found for L1, extended as in complexes **1** or **4**, kinked and S-shaped as in **3** and **5** and **7**–**9**, and C-shaped as in **11**, the molecule being centrosymmetric in the two former cases (the exceptions being found in **10** and **11**, two complexes containing several inequivalent molecules in different conformations). Consideration of Newman projections down the central C–C bond of L1 (Figure S2, Supporting Information) shows that the N–C–C–N dihedral is 180° in all cases except for three of the inequivalent zwitterion units in complex **11**, where the angles are 162, 174 and 159°, *i.e.* not greatly different. In all but one case (in **11**), the conformation adopted places the carboxylate groups remote from one another and the conformation freedom of L1 thus appears to be largely limited to the disposition of the $CH_2CO_2^-$ substituents. In contrast, L2 is of course never centrosymmetric, and only in complex **12** does it have twofold rotation symmetry; however, here also, extended (**6**) and kinked (**2**, **12**) geometries are found.

An unrelated variation of coordination mode is added to these variations in shape. The most common mode for both zwitterionic ligands is the simple μ_2-bis(κ^1O)-bridging one, in which the two carboxylate groups are monodentate, found in complexes **2**, **5**, **6** and **8**–**11**; μ_2-bridging is also found in **3**, **7**, **10**, and **11** with one of the carboxylate groups or both being κ^2O,O'-chelating. In all these cases, the zwitterionic ligand is a simple edge in the networks formed, a situation most common in previous studies with other zwitterionic ligands.[16] Only in complex **11** does one of the inequivalent L1 molecules adopt the μ_3-($\kappa^2O,O';\kappa^1O'':\kappa^1O'''$) mode

and is a 3-c node, while the higher connectivity is observed in **4** and **12** where L1 and L2, respectively, are 4-c nodes, being bound in the μ_4-bis(κ^1O:κ^1O')-bridging mode. The anionic dicarboxylates are also often 2-c, μ_2-bridges (**3**, **4**, **5**, **7**, **8**, and **11**) or even terminal (**1** and **2**), with isophthalate in **6** being the sole instance of a 3-c node. The only tetracarboxylic acid used, thftcH_4, retains one of its protons and is also a 3-c node in **9**. Notwithstanding these moderate assembling performances of the ligands, di- and triperiodic coordination polymers are obtained as a result of the large coordination number of the uranyl ion which makes it generally a 3-c or 4-c node. Only in the case of isophthalate was it possible to obtain complexes with both L1 and L2 (**3** and **6**, respectively), and they appear to be quite different, notwithstanding the only slight modification of the chain length by one carbon atom. The zwitterionic ligands are simple edges in both complexes, but ipht^{2-} is either an edge or a 3-c node, resulting in an increase of periodicity in the latter case. Although the difference thus seems to be due to the anionic ligand connectivity, the necessary change in the zwitterionic ligand symmetry (centrosymmetric in **3**, asymmetric in **6**) may however also possibly have an influence on the outcome.

The large size of the zwitterionic dicarboxylates used here as well as in previous studies allows for the formation of species with a large separation between metal ion nodes and hence large cells, which in turn is favorable for generating intricate or entangled networks. Three interesting such cases are reported here. Complex **10** displays inclusion of an elongated, linear binuclear complex within the cells of stacked **hcb** networks, complex **11** is, to the best of our knowledge, the first example in uranyl chemistry of 2D + 3D hetero-interpenetration, and complex **12** is a twofold interpenetrated triperiodic framework. An interesting point here is the tendency of tdc^{2-} in **11** to counteract mixed-ligand behaviour through self-sorting resulting in the formation of a separate diperiodic, anionic network, the cationic, triperiodic framework only including one tdc^{2-} for 7 L1 ligands, a particularly unusual situation. The synthesis of **12** does not involve any anionic carboxylate ligand and the framework includes instead undulating

chlorouranate chains as subunits, the presence of oxo and hydroxo anions being a distinctive feature of this complex within the present series, although it is quite common in uranyl ion complexes generally and adds a measure of unpredictability to already complex systems, though here it may simply be due to acid consumption in the oxidation of iodide. It is notable that, notwithstanding some entangled species incorporating polynuclear oxo-bridged uranyl clusters,[78] **12** is a unique example of an interpenetrated framework containing an extended, monoperiodic uranate subunit.

Luminescence measurements. Emission spectra under excitation at 420 nm and photoluminescence quantum yields (PLQYs) were recorded for complexes **1**–**4**, **6**, **7** and **11** in the solid state, compound **9** being non-emissive and no sufficient quantity of pure compound having been obtained for the other complexes. The PLQYs are very different for these compounds, four of them being quite strongly emissive [**1** (18%), **2** (24%), **3** (10%), and **7** (8%)], while the other three are very weakly emissive [**4** and **11** (<1%), and **6** (2%)]. The emission spectra of the complexes of the first group are given in Figure 15, while the other

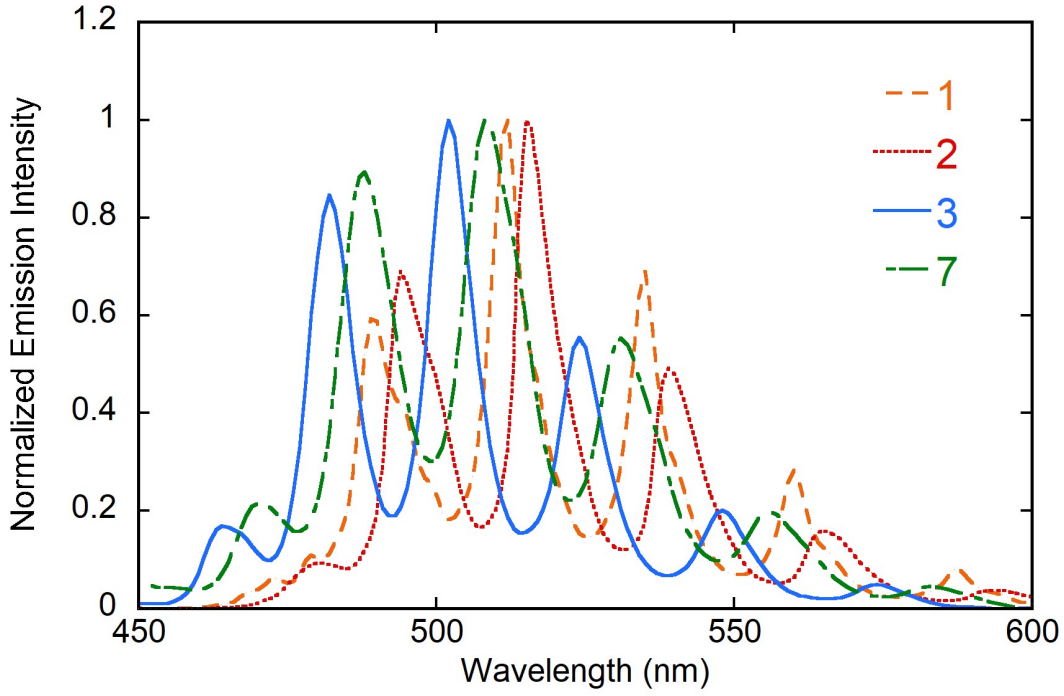

Figure 15. Emission spectra of compounds **1**, **2**, **3** and **7** in the solid state at room temperature, under excitation at a wavelength of 420 nm.

ones, which display prominently the tail of the lamp signal and are much more sensitive to the possible presence of impurities, are given in Figure S3. The common feature of complexes **4**, **6** and **11** is the presence of at least partial close stacking of aromatic units and there is some evidence that interactions in such stacks can give rise to de-excitation of U^{VI} and low-energy emission with the characteristics of an organic fluorophore.[64] Three of the most emissive complexes, and particularly the two with the highest PLQYs contain ligands of the pyridinedicarboxylate family and this comes as no surprise since these ligands have previously been shown to give complexes with strong uranyl emission, the highest PLQY measured being 71% for a complex with 2,5-$pydc^{2-}$.[62] The pyridinedicarboxylate ligands possibly favor uranyl emission through the "antenna effect" due to energy transfer from excited π electrons of the ligand to uranium.[79] In the present series, 2,4-$pydc^{2-}$ gives the most emissive complex, followed by 2,6- and 2,5-$pydc^{2-}$, the other case involving $ipht^{2-}$. In all these four cases, the fine structure visible in the well-resolved emission spectra corresponds to the vibronic progression of the $S_{11} \rightarrow S_{00}$ and $S_{10} \rightarrow S_{0\nu}$ ($\nu = 0$–4) electronic transitions.[80,81] The minor shifts in the peak positions are related to differences in the coordination number and nature of donor atoms, and the positions observed here are in very good agreement with those previously found,[82] with the most blue-shifted spectrum being that of complex **3** with a uranyl O_6 equatorial environment (four main maxima at 482, 502, 524 and 548 nm), followed by that of complex **7**, with an O_5N environment (488, 508, 531 and 556 nm), that of complex **1**, with the O_4N_2 environment (489, 512, 535 and 560 nm), and finally that of **2**, with the O_3N_2 environment (494, 515, 539 and 565 nm). The most blueshifted, weak peak corresponding to the hot-band transition[81] is more intense and better resolved in the spectra of **3** and **7** (464 and 470 nm, respectively). The peaks in the spectra of **1** and **2** display shoulders, particularly marked for **1**, such superposition of different

vibronic progressions having previously been found for other pyridinedicarboxylate uranyl complexes.[51,62,79]

CONCLUSIONS

We have reported the synthesis and crystal structure of a series of 12 uranyl ion complexes involving the diammonioacetate zwitterionic ligands L1 and L2 associated with diverse coordinating anions, mainly anionic polycarboxylates, and also oxo, hydroxo and chlorido donors. As previously found in families of complexes involving different zwitterions,[15–17] combining zwitterionic and anionic polycarboxylates most often gives the desired mixed-ligand species. There are however some anomalies here, with the protonated zwitterion being a simple counterion in **1**, the terephthalate being completely absent in **10**, and, more interestingly, the tendency of 2,5-thiophenedicarboxylate to counteract mixed-ligand behaviour through self-sorting resulting in the remarkably complicated hetero-interpenetrated structure seen in complex **11**. In addition to that of complex **11**, two cases of structurally original compounds are reported, that of complex **10** which displays the crossing of the hexanuclear cells of a diperiodic network by the linear rods formed by L1-bridged dinuclear units, and that of complex **12**, a twofold interpenetrated triperiodic framework containing chlorouranate chains as subunits. Overall, the flexibility anticipated for aliphatic linkages does not result in a very broad range of carboxylate group dispositions in the species presently characterized. Four of the complexes are strongly emissive (three of them including pyridinedicarboxylate ligands), with PLQYs between 8 and 24%, and they display well-resolved spectra with maxima positions in good agreement with the ranges usually observed in function of number and nature of donor atoms.

Acknowledgements: This work was supported by Iketani Science and Technology Foundation, TOBEMAKI Scholarship Foundation, Sasakawa Scientific Research Grant from The Japan

Science Society and KAKENHI Grant-in-Aid for Early-Career Scientists JP22K14698 for S. Kusumoto, and JSPS KAKENHI Grant Number 20K21213 for S. Hayami.

ASSOCIATED CONTENT

Accession Codes

CCDC 2225009−2225020 contain the supplementary crystallographic data for this paper. These data can be obtained free of charge via www.ccdc.cam.ac.uk/data_request/cif, or by emailing data_request@ccdc.cam.ac.uk, or by contacting The Cambridge Crystallographic Data Centre, 12 Union Road, Cambridge CB2 1EZ, UK; fax: +44 1223 336033.

Supporting Information

The Supporting Information is available free of charge at . Table S1: Elemental analysis results and yields; Figures S1–S3: ^{1}H NMR spectra of L1H_2Cl_2 and L2H_2Cl_2; Newman projections of L1; emission spectra of complexes **4**, **6**, and **11** (PDF).

AUTHOR INFORMATION

Corresponding Authors

*E-mail: hayami@kumamoto-u.ac.jp (S. H.)

*E-mail: ykim@kumamoto-u.ac.jp (Y.K.)

*E-mail: harrowfield@unistra.fr (J.H.)

*E-mail: pierre.thuery@cea.fr (P.T.)

ORCID

Sotaro Kusumoto: 0000-0002-7501-383X

Youssef Atoini: 0000-0003-4851-3713

Jee Young Kim: 0000-0001-7979-7929

Shinya Hayami: 0000-0001-8392-2382

Yang Kim: 0000-0001-8187-0793

Jack Harrowfield: 0000-0003-4005-740X

Pierre Thuéry: 0000-0003-1683-570X

Notes

The authors declare no competing financial interest.

REFERENCES

1. Furukawa, H.; Müller, U.; Yaghi, O. M. "Heterogeneity within Order" in Metal–Organic Frameworks. *Angew. Chem. Int. Ed.* **2015**, *54*, 3417–3430.
2. Pullen, S.; Clever, G. H. Mixed-Ligand Metal–Organic Frameworks and Heteroleptic Coordination Cages as Multifunctional Scaffolds–A Comparison. *Acc. Chem. Res.* **2018**, *51*, 3052−3064.
3. Viciano-Chumillas, M.; Liu, X.; Leyva-Pérez, A.; Armentano, D.; Ferrando-Soria, J.; Pardo, E. Mixed Component Metal-Organic Frameworks: Heterogeneity and Complexity at the Service of Application Performances. *Coord. Chem. Rev.* **2022**, *451*, 214273.
4. Andrews, M. B.; Cahill, C. L. Uranyl Bearing Hybrid Materials: Synthesis, Speciation, and Solid-State Structures. *Chem. Rev*. **2013**, *113*, 1121–1136.

5. Loiseau, T.; Mihalcea, I.; Henry, N.; Volkringer, C. The Crystal Chemistry of Uranium Carboxylates. *Coord. Chem. Rev.* **2014**, *266–267*, 69–109.
6. Su, J.; Chen, J. S. MOFs of Uranium and the Actinides. *Struct. Bond*. **2015**, *163*, 265–296.
7. Thuéry, P.; Harrowfield, J. Recent Advances in Structural Studies of Heterometallic Uranyl-Containing Coordination Polymers and Polynuclear Closed Species. *Dalton Trans.* **2017**, *46*, 13660–13667.
8. Lv, K.; Fichter, S.; Gu, M.; März, J.; Schmidt, M. An Updated Status and Trends in Actinide Metal-Organic Frameworks (An-MOFs): From Synthesis to Application. *Coord. Chem. Rev*. **2021**, *446*, 214011.
9. Kerr, A. T.; Cahill, C. L. Crystal Engineering with the Uranyl Cation III. Mixed Aliphatic Dicarboxylate/Aromatic Dipyridyl Coordination Polymers: Synthesis, Structures, and Speciation. *Cryst. Growth Des*. **2011**, *11*, 5634–5641.
10. Xu, W.; Si, Z. X.; Xie, M.; Zhou, L. X.; Zheng, Y. Q. Experimental and Theoretical Approaches to Three Uranyl Coordination Polymers Constructed by Phthalic Acid and N,N′-Donor Bridging Ligands: Crystal Structures, Luminescence, and Photocatalytic Degradation of Tetracycline Hydrochloride. *Cryst. Growth Des.* **2017**, *17*, 2147−2157.
11. Thuéry, P.; Atoini, Y.; Harrowfield, J. Uranyl−Organic Coordination Polymers with *trans*-1,2-, *trans*-1,4- and *cis*-1,4-Cyclohexanedicarboxylates: Effects of Bulky PPh_4^+ and PPh_3Me^+ Counterions. *Cryst. Growth Des.* **2018**, *18*, 2609−2619.
12. Thuéry, P.; Harrowfield, J. Uranyl Ion-Containing Polymeric Assemblies with *cis/trans* Isomers of 1,2-, 1,3-, and 1,4-Cyclohexanedicarboxylates, Including a Helical Chain and a 6-Fold-Interpenetrated Framework. *Cryst. Growth Des.* **2020**, *20*, 262−273.
13. Thuéry, P.; Atoini, Y.; Harrowfield, J. Structure-Directing Effects of Coordinating Solvents, Ammonium and Phosphonium Counterions in Uranyl Ion Complexes with 1,2-, 1,3-, and 1,4-Phenylenediacetates. *Inorg. Chem.* **2020**, *59*, 2503−2518.

14. Thuéry, P.; Harrowfield, J. Varying Structure-Directing Anions in Uranyl Ion Complexes with Ni(2,2′:6′,2″-terpyridine-4′-carboxylate)$_2$. *Eur. J. Inorg. Chem.* **2022**, e202200011.
15. Thuéry, P.; Harrowfield, J. Ni(2,2′:6′,2″-terpyridine-4′-carboxylate)$_2$ Zwitterions and Carboxylate Polyanions in Mixed-Ligand Uranyl Ion Complexes with a Wide Range of Topologies. *Inorg. Chem*. **2022**, *61*, 9725–9745.
16. Kusumoto, S.; Atoini, Y.; Masuda, S.; Kim, J. Y.; Hayami, S.; Kim, Y.; Harrowfield, J.; Thuéry, P. Zwitterionic and Anionic Polycarboxylates as Coligands in Uranyl Ion Complexes, and Their Influence on Periodicity and Topology. *Inorg. Chem.* **2022**, *61*, 15182−15203.
17. Kusumoto, S.; Atoini, Y.; Masuda, S.; Koide, Y.; Kim, J. Y.; Hayami, S.; Kim, Y.; Harrowfield, J.; Thuéry, P. Varied Role of Organic Carboxylate Dizwitterions and Anionic Donors in Mixed-Ligand Uranyl Ion Coordination Polymers. *CrystEngComm* **2022**, *24*, 7833–7844.
18. Groom, C. R.; Bruno, I. J.; Lightfoot, M. P.; Ward, S. C. The Cambridge Structural Database. *Acta Crystallogr., Sect. B* **2016**, *72*, 171–179.
19. Taylor, R.; Wood, P. A. A Million Crystal Structures: The Whole is Greater than the Sum of Its Parts. *Chem. Rev.* **2019**, *119*, 9427–9477.
20. Wu, D. D.; Mak, T. C. W. Mercury(II) Chloride Adducts of Flexible Double Betaines: Influence of Different Polymethylene Bridges Between the Quaternary Nitrogen Atoms. *J. Chem. Soc., Dalton Trans.* **1995**, 139–143.
21. Wu, D. D.; Mak, T. C. W. Formation of Various Polymeric Frameworks by Dicarboxylate-Like Ligands: Synthesis and Crystal Structures of Polymeric Complexes of Sodium Perchlorate with Flexible Double Betaines. *Struct. Chem*. **1996**, *7*, 91–101.
22. Wei, P. R.; Wu, D. D.; Zhou, Z. Y.; Li, S. L.; Mak, T. C. W. Lanthanide Coordination Polymers with Dicarboxylate-Like Ligands: Crystal Structures of Polymeric

Neodymium(III) and Erbium(III) Complexes with Flexible Double Betaines. *Polyhedron* **1997**, *16*, 749–763.

23. Wei, P. R.; Wu, D. D.; Zhou, Z. Y.; Mak, T. C. W. Generation of Coordination Networks with Dicarboxylate-Like Ligands: Synthesis and Crystal Structures of Polymeric Complexes of Gadolinium(III) Perchlorate with Flexible Double Betaines. *Polyhedron* **1998**, *17*, 497–505.
24. Jiang, H. L.; Makal, T. A.; Zhou, H. C. Interpenetration Control in Metal–Organic Frameworks for Functional Applications. *Coord. Chem. Rev.* **2013**, *257*, 2232–2249.
25. Batten, S. R. Interpenetration and Entanglement in Coordination Polymers. In *Metal-Organic Framework Materials, Encyclopedia of Inorganic and Bioinorganic Chemistry*, Eds. L. MacGillivray and C. M. Lukehart, Wiley, Chichester, UK, **2014**, pp. 1–16, DOI: 10.1002/9781119951438.eibc2230.
26. Gong, Y. N.; Zhong, D. C.; Lu, T. B. Interpenetrating Metal–Organic Frameworks. *CrystEngComm* **2016**, *18*, 2596–2606.
27. Chang, K. C.; Lee, L. W.; Lin, H. M.; Yen, C. F.; Wang, C. M.; Wu, J. Y. Hetero-Interpenetrating Porous Coordination Polymers. *Dalton Trans.* **2022**, *51*, 7025–7034.
28. Lloyd, A. W.; Baker, J. A.; Smith, G.; Olliff, C. J.; Rutt, K. J. A Comparison of Glycine, Sarcosine, *N,N*-Dimethylglycine, Glycinebetaine, and *N*-Modified Betaines as Liposome Cryoprotectants. *J. Pharm. Pharmacol*. **1992**, *44*, 507–511.
29. Andrews, M. B.; Cahill, C. L. *In Situ* Oxalate Formation During Hydrothermal Synthesis of Uranyl Hybrid Materials. *CrystEngComm* **2011**, *13*, 7068–7078.
30. Knope, K. E.; Kimura, H.; Yasaka, Y.; Nakahara, M.; Andrews, M. B.; Cahill, C. L. Investigation of in Situ Oxalate Formation from 2,3-Pyrazinedicarboxylate under Hydrothermal Conditions Using Nuclear Magnetic Resonance Spectroscopy. *Inorg. Chem.* **2012**, *51*, 3883–3890.

31. *APEX3 Crystallography Software Suite,* Ver. 2019.1-0; Bruker AXS: Madison, WI, 2019.

32. *SAINT,* Ver. 8.40A; Bruker Nano: Madison, WI, 2019.

33. *SADABS, Bruker/Siemens Area Detector Absorption and Other Corrections,* Ver. 2016/2; Bruker AXS: Madison, WI, 2016.

34. Krause, L.; Herbst-Irmer, R.; Sheldrick, G. M.; Stalke, D. Comparison of Silver and Molybdenum Microfocus X-Ray Sources for Single-Crystal Structure Determination. *J. Appl. Crystallogr.* **2015**, *48,* 3–10.

35. Sheldrick, G. M. SHELXT – Integrated Space-Group and Crystal-Structure Determination. *Acta Crystallogr., Sect. A* **2015**, *71*, 3–8.

36. Sheldrick, G. M. Crystal Structure Refinement with SHELXL. *Acta Crystallogr., Sect. C* **2015**, *71*, 3–8.

37. Hübschle, C. B.; Sheldrick, G. M.; Dittrich, B. *ShelXle*: a Qt Graphical User Interface for SHELXL. *J. Appl. Crystallogr.* **2011**, *44*, 1281–1284.

38. Spek, A. L. *PLATON* SQUEEZE: a Tool for the Calculation of the Disordered Solvent Contribution to the Calculated Structure Factors. *Acta Crystallogr., Sect. C* **2015**, *71*, 9–18.

39. Burnett, M. N.; Johnson, C. K. *ORTEPIII*, Report ORNL-6895; Oak Ridge National Laboratory: TN, 1996.

40. Farrugia, L. J. WinGX and ORTEP for Windows: an Update. *J. Appl. Crystallogr.* **2012**, *45,* 849–854.

41. Momma, K.; Izumi, F. *VESTA* 3 for Three-Dimensional Visualization of Crystal, Volumetric and Morphology Data. *J. Appl. Crystallogr.* **2011**, *44,* 1272–1276.

42. Blatov V. A.; Shevchenko, A. P.; Proserpio, D. M. Applied Topological Analysis of Crystal Structures with the Program Package ToposPro. *Cryst. Growth Des.* **2014**, *14*, 3576–3586.

43. Zhang, X.-M. Hydro(solvo)thermal in situ Ligand Syntheses. *Coord. Chem. Rev.* **2005**, *249*, 1201–1219.

44. Ahmad, M.; Cox, A.; Kemp, T. J.; Sultana, Q. Physical and Chemical Quenching of Excited Uranyl Ion by Organic Molecules Studied by Fluorimetric and Laser Flash Photolysis Methods. *J. Chem. Soc., Perkin Trans. 2* **1975**, 1867–1872.
45. Wu, S.; Mei, L.; Hu, K.-Q.; Chai, Z.-F.; Nie, C.-M.; Shi, W.-Q. pH-Dependent Synthesis of Octa-nuclear Uranyl-oxalate Network Mediated by U-shaped Linkers. *J. Inorg. Mater.* **2020**, *35*, 243–248.
46. Thuéry, P.; Harrowfield, J. Contrasting Networks and Entanglements in Uranyl Ion Complexes with Adipic and *trans,trans*-Muconic Acids. *Inorg. Chem.* **2022**, *61*, 2790–2803.
47. Thuéry, P.; Harrowfield, J. Stepwise Introduction of Flexibility into Aromatic Dicarboxylates Forming Uranyl Ion Coordination Polymers: a Comparison of 2-Carboxyphenylacetate and 1,2-Phenylenediacetate. *Eur. J. Inorg. Chem.* **2021**, 2182−2192.
48. Thuéry, P.; Atoini, Y.; Harrowfield, J. Crown Ethers and Their Alkali Metal Ion Complexes as Assembler Groups in Uranyl−Organic Coordination Polymers with *cis*-1,3-, *cis*-1,2-, and *trans*-1,2-Cyclohexanedicarboxylates. *Cryst. Growth Des*. **2018**, *18*, 3167−3177.
49. Immirzi, A.; Bombieri, G.; Degetto, S.; Marangoni, G. The Crystal and Molecular Structure of Pyridine-2,6-dicarboxylatodioxouranium(VI) Monohydrate. *Acta Crystallogr., Sect. B: Struct. Sci.* **1975**, *31*, 1023–1028.
50. Xu, C.; Tian, G.; Teat, S. J.; Rao, L. Complexation of U(VI) with Dipicolinic Acid: Thermodynamics and Coordination Modes. *Inorg. Chem.* **2013**, *52*, 2750−2756.
51. Harrowfield, J. M.; Lugan, N.; Shahverdizadeh, G. H.; Soudi, A. A.; Thuéry, P. Solid-State Luminescence and π-Stacking in Crystalline Uranyl Dipicolinates. *Eur. J. Inorg. Chem*. **2006**, 389–396.
52. Spackman, M. A.; Jayatilaka, D. Hirshfeld Surface Analysis. *CrystEngComm* **2009**, *11*, 19–32.

53. Wolff, S. K.; Grimwood, D. J.; McKinnon, J. J.; Turner, M. J.; Jayatilaka, D.; Spackman, M. A. *CrystalExplorer*, University of Western Australia, 2012.

54. Spek, A. L. Structure Validation in Chemical Crystallography. *Acta Crystallogr., Sect. D* **2009**, *65*, 148–155.

55. Etter, M. C.; MacDonald, J. C.; Bernstein, J. Graph-Set Analysis of Hydrogen-Bond Patterns in Organic Crystals. *Acta Crystallogr., Sect. B* **1990**, *46*, 256–262.

56. Bernstein, J.; Davis, R. E.; Shimoni, L.; Chang, N. L. Patterns in Hydrogen Bonding: Functionality and Graph Set Analysis in Crystals. *Angew. Chem. Int. Ed.* **1995**, *34*, 1555–1573.

57. Vallet, V.; Moll, H.; Wahlgren, U.; Szabó, Z.; Grenthe, I. Structure and Bonding in Solution of Dioxouranium(VI) Oxalate Complexes: Isomers and Intramolecular Ligand Exchange. *Inorg. Chem.* **2003**, *42*, 1982–1993.

58. Abraham, F.; Arab-Chapelet, B.; Rivenet, M.; Tamain, C.; Grandjean, S. Actinide Oxalates, Solid State Structures and Applications. *Coord. Chem. Rev*. **2014**, *266–267*, 28–68.

59. Cantos, P. M.; Frisch, M.; Cahill, C. L. Synthesis, Structure and Fluorescence Properties of a Uranyl-2,5-pyridinedicarboxylic Acid Coordination Polymer: The Missing Member of the UO_2^{2+}-2,n-pyridinedicarboxylic Series. *Inorg. Chem. Commun.* **2010**, *13*, 1036–1039.

60. Severance, R. C.; Cortese, A. J.; Smith, M. D.; zur Loye, H. C. Hydrothermal Synthesis, Structure, and Luminescence of a U(VI) Complex. *J. Chem. Crystallogr.* **2013**, *43*,171–177.

61. Si, Z. X.; Xu, W.; Zheng, Y. Q. Synthesis, Structure, Luminescence and Photocatalytic Properties of an Uranyl-2,5-pyridinedicarboxylate Coordination Polymer. *J. Solid State Chem.* **2016**, *239*, 139–144.

62. Thuéry, P.; Atoini, Y.; Kusumoto, S.; Hayami, S.; Kim, Y.; Harrowfield, J. Optimizing Photoluminescence Quantum Yields in Uranyl Dicarboxylate Complexes: Further

Investigations of 2,5-, 2,6- and 3,5-Pyridinedicarboxylates and 2,3-Pyrazinedicarboxylate. *Eur. J. Inorg. Chem.* **2020**, 4391–4400.

63. Thuéry, P. Uranyl–Organic Assemblies with Acetate-Bearing Phenyl- and Cyclohexyl-Based Ligands. *Cryst. Growth Des.* **2011**, *11*, 347–355.
64. Thuéry, P.; Atoini, Y.; Harrowfield, J. Functionalized Aromatic Dicarboxylate Ligands in Uranyl–Organic Assemblies: The Cases of Carboxycinnamate and 1,2-/1,3-Phenylenedioxydiacetate. *Inorg Chem.* **2020**, *59*, 2923–2936.
65. Weissman, S. A.; Zewge, D. Recent Advances in Ether Dealkylation. *Tetrahedron* **2005**, *61*, 7833–7863.
66. Joshi, A. V.; Baidoosi, M.; Mukhopadhyay, S.; Sasson, Y. Nitration of Phenol and Substituted Phenols with Dilute Nitric Acid using Phase-Transfer Catalysts. *Org. Proc. Res. Dev.* **2003**, *7*, 95–97.
67. Chan, E. J.; Grabowsky, S.; Harrowfield, J. M.; Shi, M. W.; Skelton, B. W.; Sobolev, A. N.; White, A. H. Hirshfeld Surface Analysis of Crystal Packing in Aza-aromatic Picrate Salts. *CrystEngComm* **2014**, *16*, 4508–4538.
68. Thuéry, P.; Harrowfield, J. Tetrahydrofurantetracarboxylic Acid: An Isomerizable Framework-Forming Ligand in Homo- and Heterometallic Complexes with UO_2^{2+}, Ag^{+}, and Pb^{2+}. *Cryst. Growth Des.* **2016**, *16*, 7083−7093.
69. Zhang, L.; Zhang, J.; Li, Z. J.; Qin, Y. Y.; Lin, Q. P.; Yao, Y. G. Breaking the Mirror: pH-Controlled Chirality Generation from a *meso* Ligand to a Racemic Ligand. *Chem. Eur. J.* **2009**, *15*, 989–1000.
70. Brammer, L.; Bruton, E. A.; Sherwood, P. Understanding the Behavior of Halogens as Hydrogen Bond Acceptors. *Cryst. Growth Des.* **2001**, *1*, 277−290.
71. Taylor, R. It Isn't, It Is: The C−H···X (X = O, N, F, Cl) Interaction Really Is Significant in Crystal Packing. *Cryst. Growth Des.* **2016**, *16*, 4165−4168.

72. Thuéry, P.; Harrowfield, J. 2,5-Thiophenedicarboxylate: An Interpenetration-Inducing Ligand in Uranyl Chemistry. *Inorg. Chem.* **2021**, *60*, 9074−9083.

73. Li, H. H.; Zeng, X. H.; Wu, H. Y.; Jie, X.; Zheng, S. T.; Chen, Z. R. Incorporating Guest Molecules into Honeycomb Structures Constructed from Uranium(VI)-Polycarboxylates: Structural Diversities and Photocatalytic Activities for the Degradation of Organic Dye. *Cryst. Growth Des*. **2015**, *15*, 10–13.

74. Thangavelu, S. G.; Butcher, R. J.; Cahill, C. L. Role of N-Donor Sterics on the Coordination Environment and Dimensionality of Uranyl Thiophenedicarboxylate Coordination Polymers. *Cryst. Growth Des*. **2015**, *15*, 3481–3492.

75. Thuéry, P.; Harrowfield, J. Counter-Ion Control of Structure in Uranyl Ion Complexes with 2,5-Thiophenedicarboxylate. *CrystEngComm* **2016**, *18*, 1550–1562.

76. Jennifer, S. J.; Jana, A. K. Influence of Pyrazine/Piperazine Based Guest Molecules in the Crystal Structures of Uranyl Thiophene Dicarboxylate Coordination Polymers: Structural Diversities and Photocatalytic Activities for the Degradation of Organic Dye. *Cryst. Growth Des*. **2017**, *17*, 5318–5329.

77. Blatov, V. A.; Carlucci, L.; Ciani, G.; Proserpio, D. M. Interpenetrating Metal–Organic and Inorganic 3D Networks: a Computer-Aided Systematic Investigation. Part I. Analysis of the Cambridge Structural Database. *CrystEngComm* **2004**, *6*, 377–395.

78. An, S. W.; Mei, L.; Hu, K. Q.; Xia, C. Q.; Chai, Z. F.; Shi, W. Q. The Templated Synthesis of a Unique Type of Tetra-Nuclear Uranyl-Mediated Two-Fold Interpenetrating Uranyl–Organic Framework. *Chem. Commun.* **2016**, *52*, 1641–1644.

79. Frisch, M.; Cahill, C. L. Synthesis, Structure and Fluorescent Studies of Novel Uranium Coordination Polymers in the Pyridinedicarboxylic Acid System. *Dalton Trans.* **2006**, 4679–4690.

80. Brachmann, A.; Geipel, G.; Bernhard, G.; Nitsche, H. Study of Uranyl(VI) Malonate Complexation by Time Resolved Laser-Induced Fluorescence Spectroscopy (TRLFS). *Radiochim. Acta* **2002**, *90*, 147–153.

81. Demnitz, M.; Hilpmann, S.; Lösch, H.; Bok, F.; Steudtner, R.; Patzschke, M.; Stumpf, T.; Huittinen, N. Temperature-dependent Luminescence Spectroscopic Investigations of Uranyl(VI) Complexation with the Halides F^- and Cl^-. *Dalton Trans*. **2020**, *49*, 7109–7122.

82. Thuéry, P.; Harrowfield, J. Structural Consequences of 1,4-Cyclohexanedicarboxylate Cis/Trans Isomerism in Uranyl Ion Complexes: from Molecular Species to 2D and 3D Entangled Nets. *Inorg. Chem.* **2017**, *56*, 13464−13481.

For Table of Contents Use Only

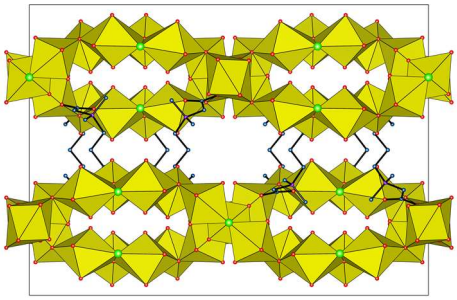

Two diammonioacetates of differing lengths were combined with anionic ligands, mainly polycarboxylates, to give a series of 12 uranyl ion complexes displaying the whole range of periodicity, from zero to three. Two examples of interpenetration have been found, one of triperiodic frameworks and the other of components of different composition and periodicity.